AN ABSTRACT OF THE THESIS OF

DAVID BRIAN KREITLOW for the degree of MASTER OF SCIENCE

in MECHANICAL ENGINEERING presented on June 6, 1977

TITLE: Geothermal Well Downhole Heat Exchanger Design Analysis

Abstract approved: _____
Dr. Gordon M. Reistad

The low temperature geothermal resource at Klamath Falls, Oregon is widely used for heating buildings. A common technique for using this resource consists of a heat exchanger down in the well inside a casing which extends the full length of the well. Slots are cut in the casing to allow circulation of the geothermal water into the casing and past the downhole heat exchanger. This results in thermosyphoning between the inside and outside of the casing.

Mathematical models of thermosyphoning through the well casing were developed for both with and without downhole heat exchanger present. Results of the model without heat exchanger present showed that thermosyphoning is sufficient to account for observed flow rates through the casing. Model results with heat exchanger included show the substantial influence of thermosyphoning on heat transfer rates and indicate several promising approaches to maximizing output.

Because of the importance of scaling and corrosion on the success of a downhole heat exchanger installation, a study of available literature on scaling and corrosion relevant to downhole heat exchangers in low temperature geothermal systems was made and recommendations for corrosion control were developed. Scaling was not deemed severe enough to justify available control measures.

GEOTHERMAL WELL DOWNHOLE HEAT EXCHANGER DESIGN ANALYSIS

by

David Brian Kreitlow

A THESIS

submitted to

Oregon State University

in partial fulfillment of
the requirements for the
degree of

MASTER OF SCIENCE

Completed June 6, 1977
Commencement June 1978

APPROVED:

Redacted for Privacy

Associate Professor of Mechanical Engineering
in charge of major

Redacted for Privacy

Head of Department of Mechanical Engineering

Redacted for Privacy

Dean of Graduate School

Date thesis is presented June 6, 1977

Thesis typed by THE COPY SHOP FOR DAVID BRIAN KREITLOW

ACKNOWLEDGEMENTS

The author wishes to express appreciation for the generous help, support and valuable advice of Dr. Gordon M. Reistad.

He also wishes to express gratitude to Dr. William McMullen, for valuable suggestions and generosity in loaning books from his personal library.

Additional thanks are due Ron Adams, for many valuable discussions of heat transfer and fluid mechanics problems related to this project, and Ed Meyer, for support of the numerical analysis involved.

Last of all, gratitude to the Energy Research Development Administration, whose financial support made this work possible.

TABLE OF CONTENTS

LIST OF FIGURES

LIST OF TABLES

NOMENCLATURE

A - total area of DHE under water

A_c - surface area of cas ing

A_i - cross sectional area inside the casing

A_o - cross sectional area of outer annulus

A_w - well wall temperature gradient

C_{ij} - constant relating pressure and mass flow rate (network model)

C_p - specific heat at constant pressure

D_h - diameter of heat exchanger pipe

DHE - downhole heat exchanger

D_i - inside diameter of casing

D_w - diameter of wellbore

De_i - hydraulic diameter of inside the casing

De_o - hydraulic diameter of annulus outside the casing

f_{fi} - Fanning friction factor for inside of casing

f_{fo} - Fanning friction factor for outer annulus

g - acceleration due to gravity

HR_{ij} - heat flux to path ij

k - thermal conductivity

L - Length of well between perforation levels

LMTD - log mean temperature difference

$\dot{m}$ - mass flow rate through casing

$\dot{m}_h$ - mass flow rate through heat exchanger

M_{ij} - mass flow rate from node i to node j (network model)

P_i - pressure on node i (network model)

Pr - Prandtl number = $\frac{C_p}{k}$

Q - thermal output of heat exchanger

r - fraction of flow through casing that is recirculated

S - flow rate of source

S_i - mass flow rate of source at node i (network model)

T_b - temperature of source (reservoir)

T_i - water temperature inside the casing

T_o - water temperature outside the casing

T_1 - water temperature in entering leg of heat exchanger for differential equation model

T_2 - water temperature in leaving leg of heat exchanger for differential equation model

T_j - water temperature at node j for network model

U_h - overall heat transfer coefficient through heat exchanger

U_i - overall heat transfer coefficient through the casing

U_w - overall heat transfer coefficient to well wall

w_1 - constant in network convection equation

$$= \frac{2f_{fi}}{\rho^2 g A_1^2 De_i \beta}$$

w_2 - constant in network convection equation

$$= \frac{2f_{fo}}{\rho^2 g A_o^2 De_o \beta}$$

β - thermal expansion coefficient

μ - viscosity

ρ - density

GEOTHERMAL WELL DOWNHOLE HEAT EXCHANGER DESIGN ANALYSIS

1. INTRODUCTION

The low temperature geothermal resource of Klamath Falls, Oregon is widely used. Culver, Lund and Svanevik (1974) state that there are approximately 400 hot water wells in the Klamath Falls area which are used to heat approximately 500 buildings, including homes, churches, and schools. The principal technique for geothermal energy recovery at Klamath Falls is the downhole heat exchanger (DHE) using city water in the loop.

Figure 1.1 shows a typical DHE installation. The important parts of the installation are: (i) the wellbore, generally 15-36 cm in diameter; (ii) a casing, which extends the full depth of the well and is approximately 5 to 10 cm smaller in diameter than the wellbore; and (iii) the DHE, which consists of a U-shaped loop of black iron pipe, usually 3 to 5 cm in diameter, extending to near the well bottom. The hot water in the well comes from a porous layer of rock near the well bottom. Slots are cut in the casing at two or more levels to allow circulation of hot water into the casing. These slots allow thermosyphoning between the inside and outside of the casing which has a major effect on heat transfer and will therefore be examined in detail in this thesis. Wells range in depth from 30 to 550 meters. Wells for heating residences are typically 60 to 90 meters deep. The deeper wells are primarily

used for heating schools and commercial establishments.

The DHE has several advantages over other methods of geothermal energy recovery: (i) no environmental problems due to disposal of geothermal water since the water never leaves the ground; (ii) corrosion problems are minimized since corrosive geothermal waters come in contact only with the heat exchanger; and (iii) depletion of groundwater supplies is not a problem since the water is not removed. The primary disadvantage of the DHE is that the thermal output of the well is generally less when a DHE is used that if hot geothermal water is pumped directly to the point of use.

Improvements in hot well technology have occured through trial and error since the first wells were dug about 1900. Early wells were cased only for a short distance near the surface to prevent caving and the influx of cold surface water. Extension of the casing has resulted in greatly increased life and increased output due to thermosyphoning through the casing. Between 1920 and 1932 plunger pumps were used on wells. In 1929 the first DHE relying on thermosyphoning for flow through the loop was installed, which is now a widely used technique. The difference in density between the cold entering water in the inlet leg of the DHE and the hot water in the outlet leg induces motion in the water: rates of 57 to 95 liters/min have been reported (Culver, Lund and Svanevik, 1974). This makes a pump unnecessary for many applications. The analysis here models the heat transfer in the

well and investigates the effects of varying parameters and methods of increasing DHE output.

Corrosion and scaling are of major importance in many geothermal applications. Scaling severity with some brines can result in blockage of pipes in 50 hours (Owen, 1976). Luckily, corrosion and scaling are much less of a problem at Klamath Falls and in other low temperature systems. However, it is still a significant factor in the economics of geothermal heating, and becomes more important as attempts are made to increase the effectiveness of geothermal heat exchangers. Because of the importance of these topics, this thesis includes a discussion of corrosion, scaling, and recommendations for corrosion control.

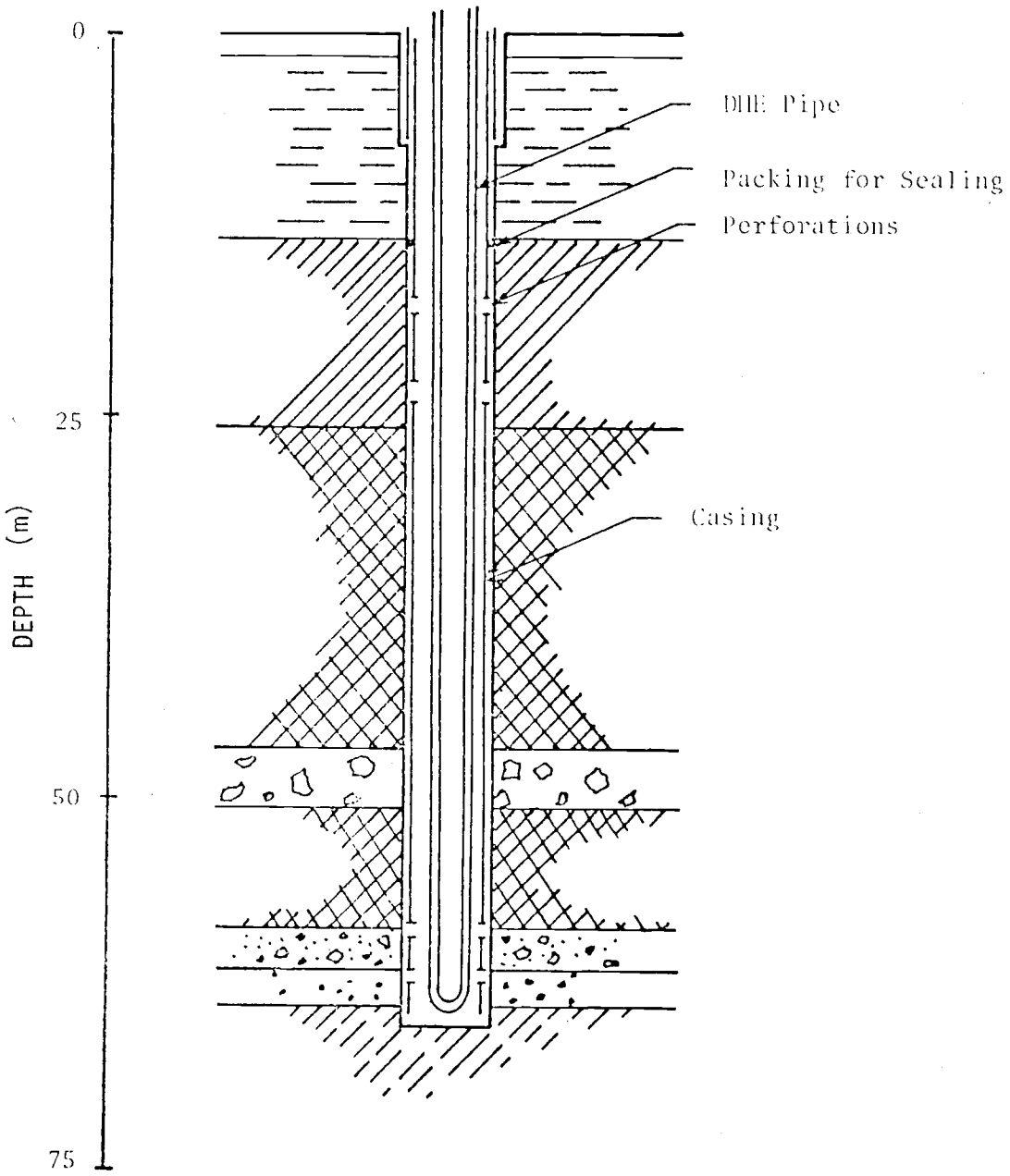

FIGURE 1.1. Typical downhole heat exchanger installation.

2. THERMOSYPHONING MODELS

Three thermosyphoning models are developed. The first model is for thermosyphoning in the cased well with no DHE. This thermosyphoning is due to conduction through the wall. Conservation of energy results in two simultaneous ordinary differential equations and momentum considerations lead to an algebraic equation. These equations lead to a single equation which is solved for the mass flow rate. Once this is known, all other quantities of interest can be calculated.

The second model includes a DHE. An energy balance leads to a two point boundary value problem with four simultaneous ordinary differential equations. Parameters of the differential equation are dependent on the unknown mass flow rate through the casing. Momentum considerations lead to an equation for the mass flow rate in terms of the integral of the unknown temperature difference between the inside and outside of the casing. This problem was solved numerically using the computer program listed in Appendix A.

The differential equation model gives reasonably good results but is rather cumbersome. Since several questions dealing with the limitations of DHEs require coupling the DHE to other systems, an effort was made to develop a much simpler model suitable for this purpose as well as to investigate the effects of mixing at the bottom of the well, which is ignored in the other models.

The result of this effort is a set of simple models which model the fluid flow and heat conduction as a network of paths and nodes, the paths for fluid flow being modelled as flow through conduits. The result of this formulation is a set of simultaneous algebraic equations. The author believes that this approach can be readily extended to include the effects of the aquifier flow and thermosyphoning in the DHE, though that is beyond the scope of this thesis.

2.1 THERMOSYPHONING IN THE WELL WITHOUT DHE

The direction and rate of fluid flow in the wells and aquifers at Klamath Falls is unknown. Well drillers believe that there are substantial horizontal flows through the aquifers (Churchill, Culver, and Reistad, 1977). Sass and Sammel (1976) state that vertical flows in the wells are probable. An experimental program is underway to make measurements in the wells to determine bulk fluid flows. Preliminary measurements (Churchill, et al., 1977) show substantial vertical flows in the cased wells (one to five cm/s) while vertical flows in the uncased wells are generally insufficient to activate the vane anemometer used for measurements, which has a sensitivity of approximately .2 cm/s. These results lead to the question of whether thermosyphoning between the inside and outside of the casing due to the temperature gradient of the wall is sufficient to account for the large observed flow rates.

A mathematical model was constructed to answer this question and to determine the effects of various parameters on the mass flow rate.

The driving force for this thermosyphoning comes from the temperature gradient of the well wall. The casing apparently serves to isolate the upward and downward flows. This results in greatly increased flow rates and a nearly uniform temperature profile inside the casing after the well is cased (Figure 2.1).

The simplified physical model consists of two concentric vertical impermeable cylinders representing the well and casing. The bottoms of the two cylinders are assumed to open into a relatively open reservoir. Near the top of the cylinders, which corresponds to the water level in the well, the inner cylinder has perforations that allow fluid to flow either to or from the outer cylinder.

The model was analyzed by assuming fluid properties and velocity to vary only in the vertical direction for both the inner pipe and for the annulus. Application of mass continuity, energy, and momentum laws then leads to the two simultaneous ordinary differential equations below, which can be solved in terms of the unknown mass flow rate assuming that the wall temperature is known:

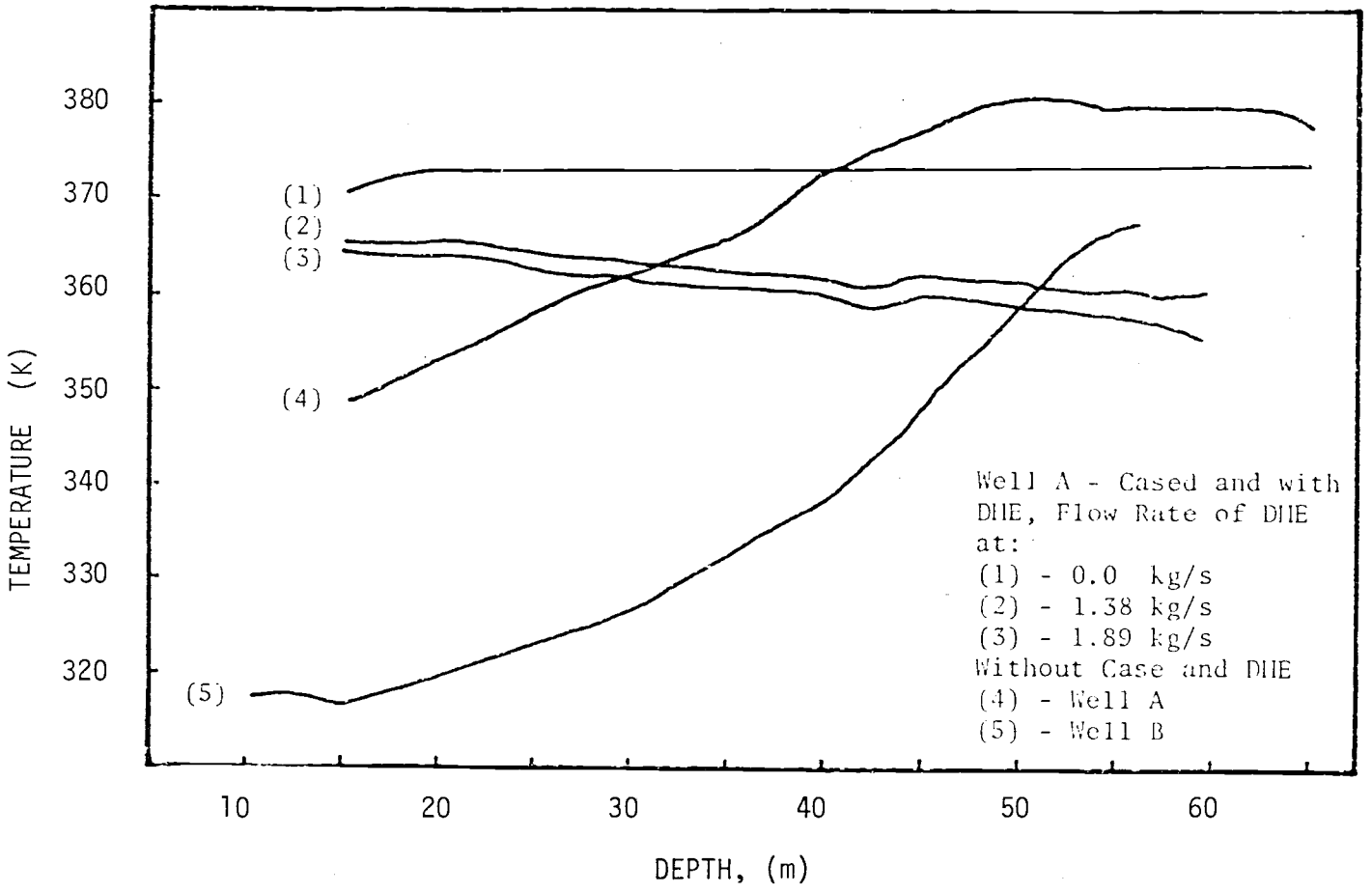

FIGURE 2.1. Measured temperature profiles of cased and uncased wells. (Values are inside the casing for the cased wells.)

$$\frac{dT_o}{dx} = \frac{U_w \pi D_w}{C_p \dot{m}} (T_o - T_w) + \frac{U_i \pi D_i}{\dot{m} C_p} (T_o - T_i) \qquad (1)$$

$$\frac{dT_i}{dx} = \frac{U_i \pi D_i}{\dot{m} C_p} (T_o - T_i) \qquad (2)$$

where the subscripts i, o, and w refer to inside, outside and wall respectively. The boundary conditions are:

$$(i) \quad T_i(0) = T_b \qquad (3)$$

$$(ii) \quad T_o(L) = T_i(L) \qquad (4)$$

The heat transfer coefficients are evaluated by the Prandtl analogy. The mass flow rate is determined by equating the head resulting from the density differences between the outside and the inside of the casing to the losses due to friction. This results in an algebraic equation which is solved iteratively for the mass flow rate.

$$\dot{m} - \frac{\rho^2 g\beta}{2C_1 L \left(\frac{f_{fi}}{A_i^2 De_i} + \frac{f_{fo}}{A_o^2 De_o}\right)} \left[B_1 (1-e^{\lambda_1 L}) + B_2 (1-e^{\lambda_2 L}) + A_w L\right] = 0 \qquad (5)$$

where

$$C_1 = \frac{U_i \pi D_i}{C_p}$$

$$C_2 = \frac{U_w \pi D_w}{C_p}$$

$$\lambda_1 = \frac{C_2 + (C_2^2 + 4C_1 C_2)^{1/2}}{2\dot{m}}$$

$$\lambda_2 = \frac{C_2 - (C_2^2+4C_1C_2)^{1/2}}{2\dot{m}}$$

and

$$B_1 = \frac{-A_w[1 + \frac{\dot{m}}{C_1}\lambda_2 e^{\lambda_2 L}]}{\lambda_2 e^{\lambda_2 L} - \lambda_1 e^{\lambda_1 L}}$$

$$B_2 = \frac{A_w[1 + \frac{\dot{m}}{C_1}\lambda_1 e^{\lambda_1 L}]}{\lambda_2 e^{\lambda_2 L} - \lambda_1 e^{\lambda_1 L}}$$

The temperature profiles can then be calculated from:

$$T_i(x) = B_1 e^{\lambda_1 x} + B_2 e^{\lambda_2 x} + \frac{A_w}{C_1}\dot{m} + T_b - A_w x \qquad (6)$$

$$T_o(x) = T_i(x) + \dot{m}/C_1(B_1\lambda_1 e^{\lambda_1 x} + B_2\lambda_2 e^{\lambda_2 x} - A_w) \qquad (7)$$

The wall temperature profile for this analysis is taken to be approximately that of the water temperature profile of the uncased well (assumed linear). The validity of this assumption depends on the location of aquifers, variations in thermal conductivity, and time. It is felt that the approximation accurately indicates trends and gives reasonable estimates of temperatures and flow rates. The thermal conductivity of the surrounding rock is considered by introducing an annular ring outside the well through which the energy must diffuse, and calculating an overall heat transfer coefficient based on this and the film coefficient.

The model ignores any mixing of the hot upgoing center fluid and the colder fluid moving downward in the annulus outside the casing that may take place at the bottom of the well. A model to examine mixing effects is discussed later.

The model results for vertical mass flowrate through the well of varying: (i) D/e (1/ the relative roughness) for the annulus; (ii) inside diameter; (iii) wall temperature gradient; and (iv) conduction distance, the thickness of the annual ring outside the well at which point the wall temperature gradient is assumed to exist (and through which the energy entering or leaving the well at the walls must be conducted) are illustrated in Figure 2.2. The results are presented for parameter variations about two standard values. The standard parameter sets, I and II are tabulated in Table 2.1 and denoted by solid and broken lines respectively in Figure 2.2. These curves show that the flow rate is quite dependent on the inside diameter and the assumed values of D/e, conduction distance, and the wall temperature gradient. The conduction distance has the greatest influence of these assumed values.

The conduction distance effectively shows the effect of time. As the conduction distance increases, conditions approach steady state. The one-dimensional conduction model is no longer valid for a conduction distance of more than a few meters, since the vertical temperature gradient is then of the same magnitude as the horizontal temperature gradient.

TABLE 2.1. Test well characteristics and standard parameters sets.

GENERAL CHARACTERISTICS

D_w = 0.254 m

D_n = 0.0508 m

Static Water Level - 14 m

Performation Levels: [17 to 22 m and
[57 to 65 m

Temperature at bottom of well = 100°C

STANDARD PARAMETER SET WITHOUT DHE	I	II
D_i =	0.203m	0.203m
D/e for outer annulus =	50	50
D/e inside casing =	3000	3000
Conduction Distance =	0	0.1 m
Wall Temperature Gradient =	0.525°/m	0.525°C/m
L for cased well	40m	40m

STANDARD PARAMETER SET WITH DHE

As above except for:

Conduction Distance = 1m

Inlet Temperature to DHE = 50°C

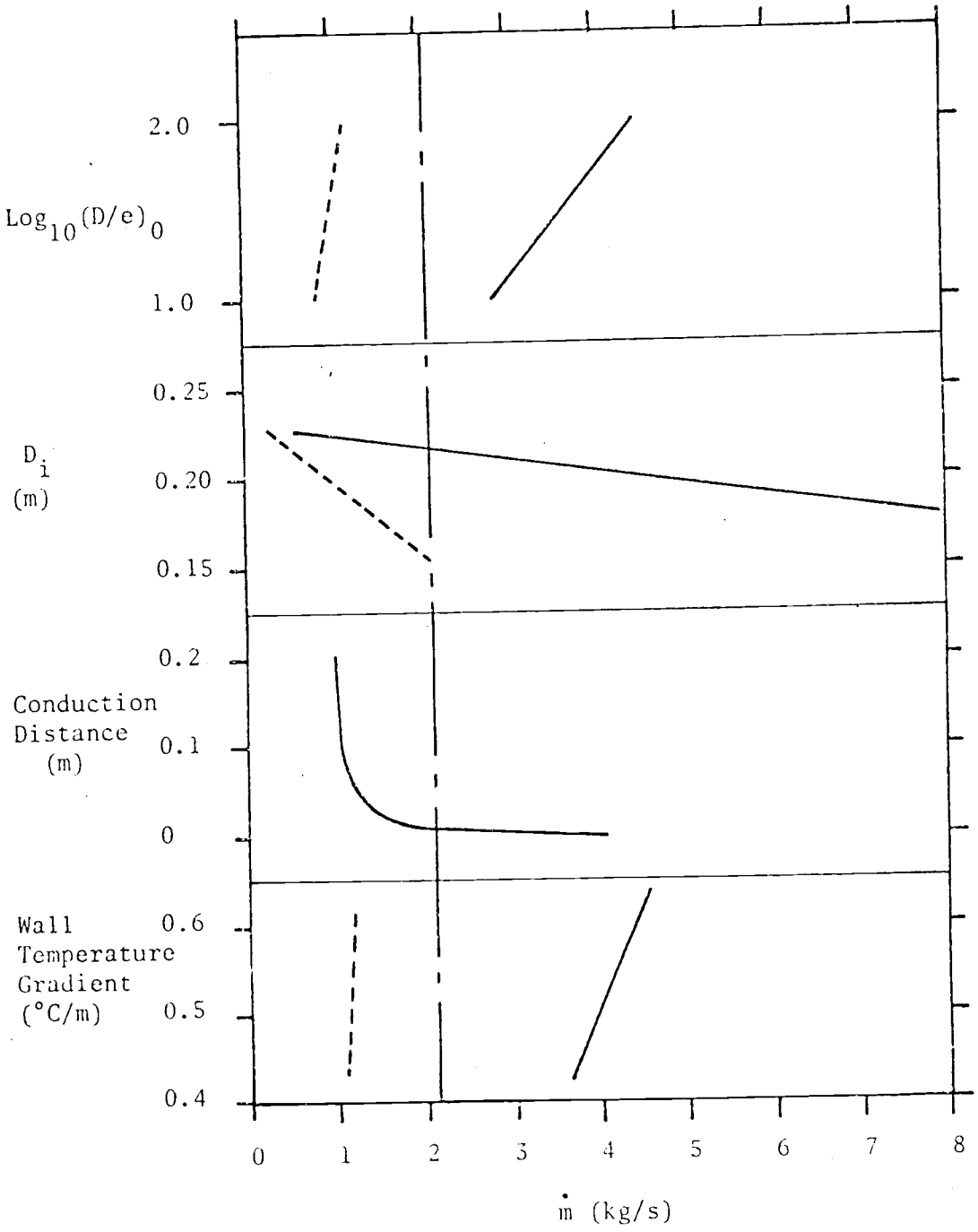

FIGURE 2.2. Model results, no DHE. Mass flow rate for various parameter variations about standard set I, ———; and standard set II, ---; (see Table 2.1) — – — Experimental value for actual well with physical characteristics of well specified in Table 2.1.

The two standard sets of parameters give results on both sides of the observed mass flow rate which supports the validity of the model. The vertical temperature profile on the inside of the casing is nearly constant as experimentally observed. (Figure 2.3)

2.2 THERMOSYPHONING WITH DHE

Early wells at Klamath Falls were not cased except for a short length near the ground surface. Later it was discovered that casing the well appreciably extends its life. Some wells that were not originally cased have been cleaned out and a casing installed. This resulted in significantly increased heat exchanger output but it was not clear how much of this was due to the casing and how much was due to the cleaning (Culver, et al., 1974). The preliminary measurements shown in Figure 2.4 indicate that the output of a well can be nearly doubled by the installation of a slotted casing. Thus the slotted casing plays a major role in efforts to increase the effectiveness of downhole heat exchangers for these applications.

The model for the cased well was extended to include a downhole heat exchanger. This results in four differential equations rather than two equations as in (1) and (2) above:

$$\frac{dT_o}{dx} = \pm \left[\frac{U_w \pi D_w}{C_p} (T_o - T_w) + \frac{U_i \pi D_i}{C_p} (T_o - T_i) \right] / \dot{m} \qquad (8)$$

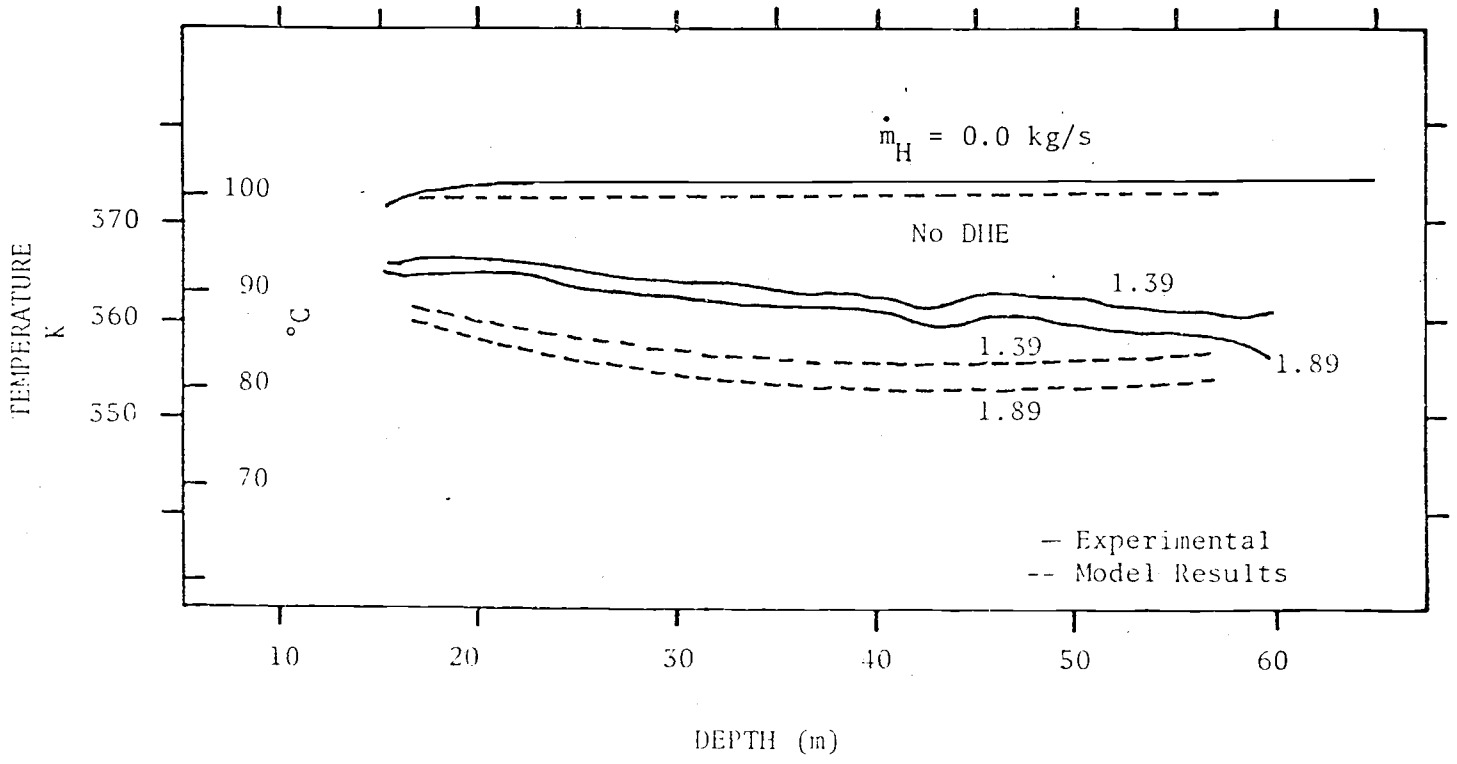

Figure 2.3. Temperature profile comparison, model and experimental results.

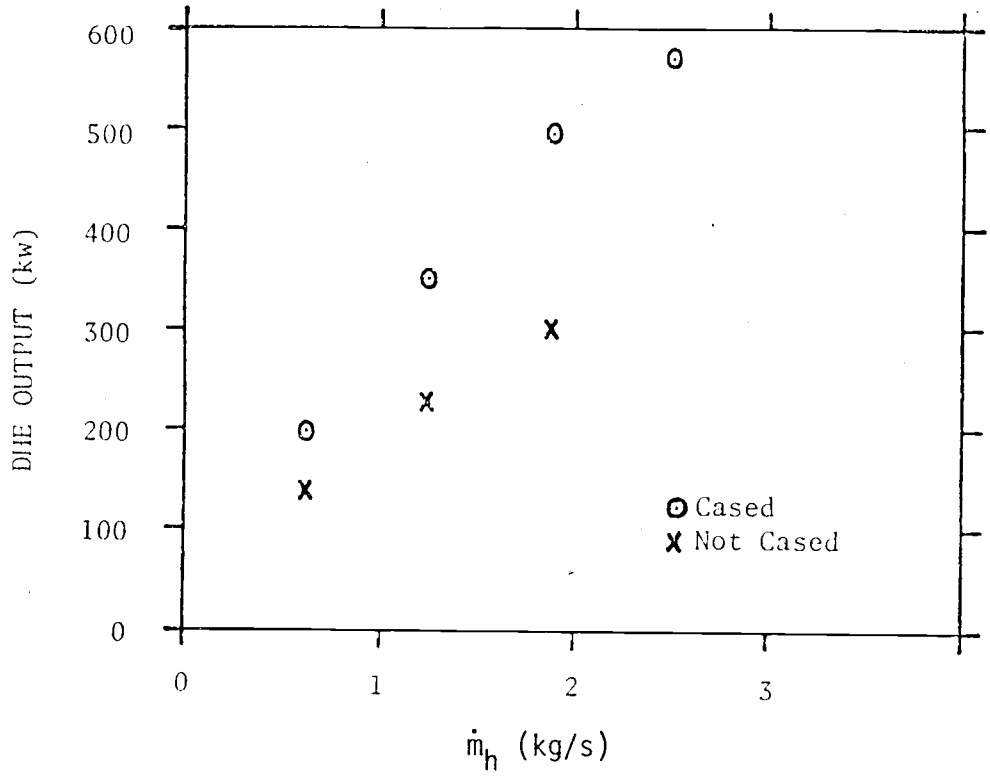

FIGURE 2.4. Measured well output.

$$\frac{dT_i}{dx} = \pm \left[\frac{U_i \pi D_i}{C_p} (T_o - T_i) - \frac{U_h \pi D_h}{C_p} (T_1 + T_2 - 2T_i)\right]/\dot{m} \qquad (9)$$

$$\frac{dT_1}{dx} = \frac{U_h \pi D_h}{C_p \dot{m}_h} (T_1 - T_i) \qquad (10)$$

$$\frac{dT_2}{dx} = \frac{U_h \pi D_h}{C_p \dot{m}_h} (T_i - T_2) \qquad (11)$$

where subscripts are as above and subscripts 1 and 2 refer to the entering and leaving legs of the heat exchanger, and subscript h refers to the heat exchanger.

The boundary conditions are

(i) $T_o(0) = T_b$ or $T_i(0) = T_b$

(ii) $T_o(L) = T_i(L)$

(iii) $T_1(0) = T_2(0)$

(iv) $T_1(L) = T_{in}$

These correspond to: (i) the temperature of the reservoir (assumed known); (ii) temperatures of the water inside and outside the casing are equal at the top of the well; (iii) the temperatures in the two legs of the heat exchanger are equal at the bottom where they join; and (iv) the temperature of the water entering the downhole heat exchanger (assumed known). These equations were solved numerically, iterating on the mass flow rate. (see Appendix A).

The mass flow rate is again determined by setting the head due to the density differences between the outside and the inside of the casing equal to the frictional loss, which results in an integral equation. The heat transfer coefficients are determined by the Prandtl analogy.

An interesting result of the model is shown in Figure 2.5. This figure shows the results of varying the length between perforations in the casing. Note that the maximum output occurs for a length of approximately 45 meters when other parameters are as in the standard parameter set, Table 2.1. The output is small for short lengths, as expected because of the small heat transfer area. As the length increases, area increases, which increases output. When the length becomes sufficiently great, however, the friction effects on the fluid column become more important and the vertical mass flow rate through the casing decreases, decreasing the thermal output.

In a real well, this effect would be less pronounced, since a significant part of the DHE is in contact with water outside the region between slots, and this would tend to flatten the curve somewhat. The actual location of the maximum depends strongly on the assumed value of D/e for the outside annulus and the flow area of the outside annulus.

In Figure 2.6, the effect of the conduction distance is shown. As previously discussed, the conduction distance essentially shows the effect of time as the region surrounding the well comes into thermal equilibrium with the well water.

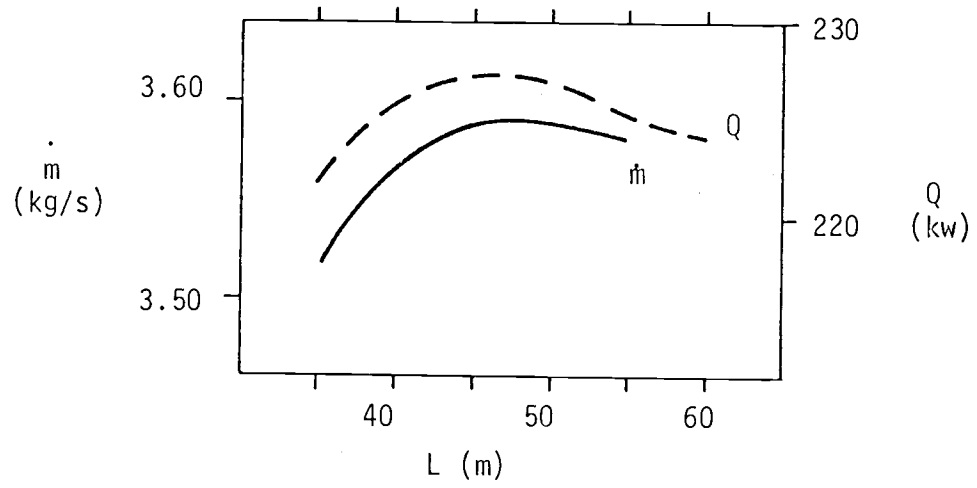

Figure 2.5. Effect of length on model results.

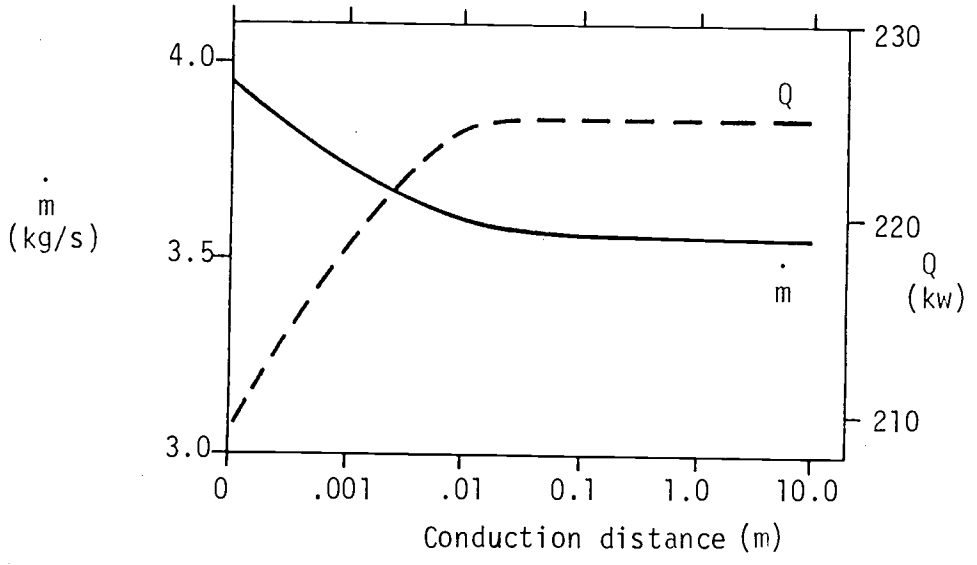

Figure 2.6. Effect of conduction distance on model results.

It can be seen from the diagram that the effect of the conduction distance is negligible beyond 0.1 meters. After an initial startup period, the effect of conduction through the wall is negligible.

The effect of the assumed value of D/e for the outer annulus is shown in Figure 2.7. The smoother the surface, the greater the mass flow rate through the casing and the greater the thermal output. This parameter is important because it has a large effect on model results and is difficult to estimate accurately, since it depends on the "roughness" of the sediments and rock that compose the well walls. The "standard" value of 50 for D/e is estimated from values for rough concrete. This value is expected to change somewhat with time as material sloughs off the well walls. Changes in this parameter do not appreciably influence the trends predicted by the model, however.

The casing diameter has considerable influence on DHE output and mass flow rate through the casing, as indicated in Figure 2.8. For maximum output it is important to provide sufficient cross sectional area for the flow outside the casing. For the standard set of parameters, the output is relatively independent of the casing diameter when it is in the range of .14 to .18 meters, but it falls off quickly for a casing diameter greater than .19 meters. If caving of the well wall is not a serious problem it is clearly advantageous to use a casing somewhat smaller than is usual.

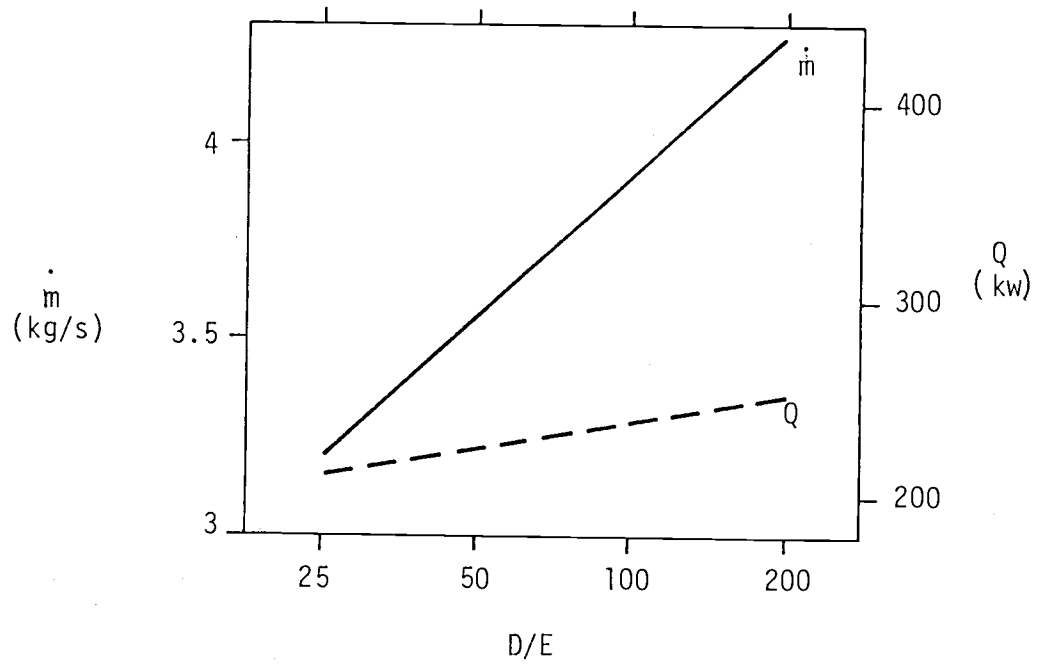

Figure 2.7. Effect of roughness of the outer annulus

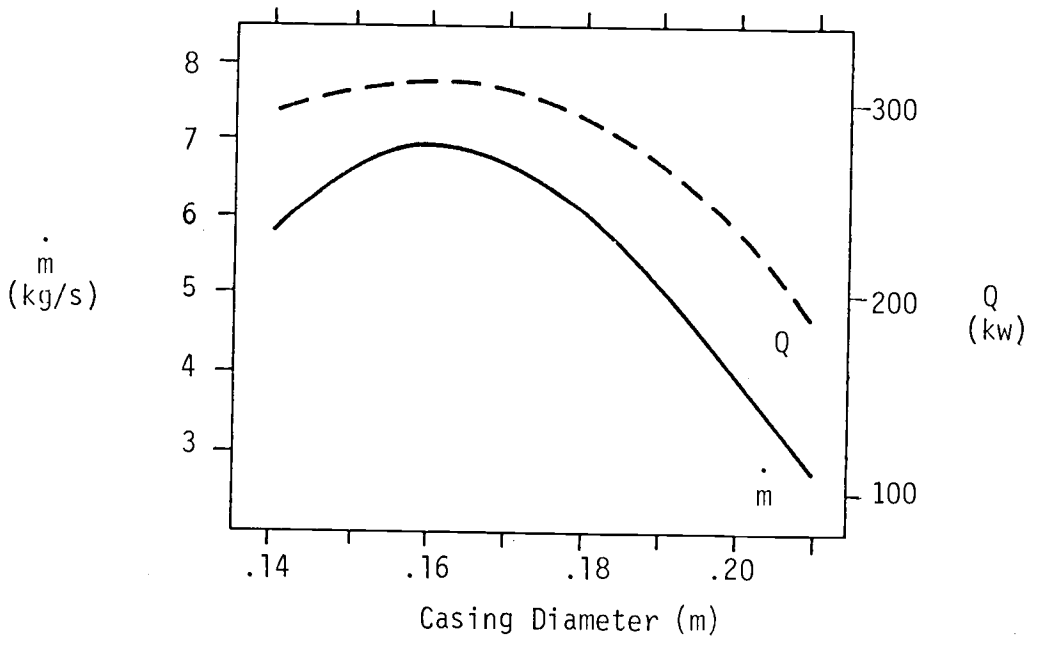

Figure 2.8. Effect of casing diameter

Figure 2.9 shows the effect of changing the mass flow rate through the heat exchanger. It can be seen that increasing the mass flow rate increases the output, but the output temperature decreases, as expected. Values of one or two kg/s through the DHE are typical for thermosyphoning DHEs (no forcing pump).

The inlet temperature naturally has an effect on the outlet temperature and mass flow rate through the casing as shown in Figure 2.10. The relationship is essentially linear in the region shown.

When results of the model are compared to the experimental test results shown in Figure 2.11, it can be seen that the model tends to give results that are somewhat low. Some discrepancy is to be expected because of the neglect of the portion of the DHE not between perforations. This could account for much of the difference. Overall, the agreement is good considering the number of estimated parameters.

2.3 Network Models

Experience gained with the differential equation model above shows that many nonlinearities can be neglected and this leads to the simple models of geothermal well systems discussed below.

These models are based on modelling the DHE-well-aquifer system as a network. There are two types of flow in the network: fluid flow (which also transports thermal energy), and heat flow (conduction) alone. Nodes are connected by paths through which

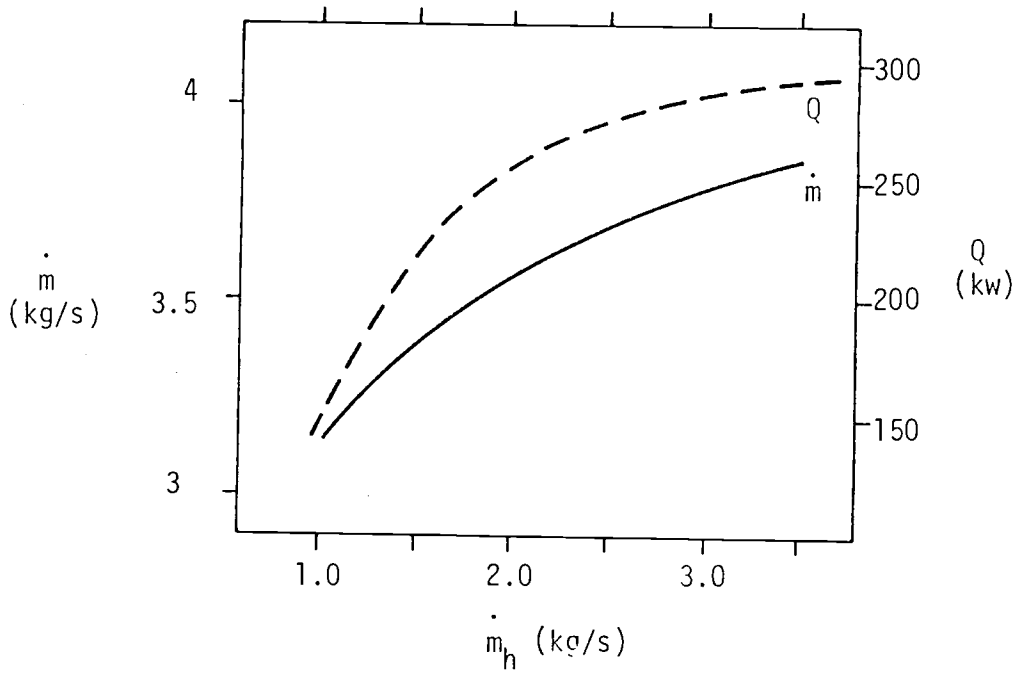

Figure 2.9. Effect of mass flow rate through heat exchanger. Inlet temperature 50°C.

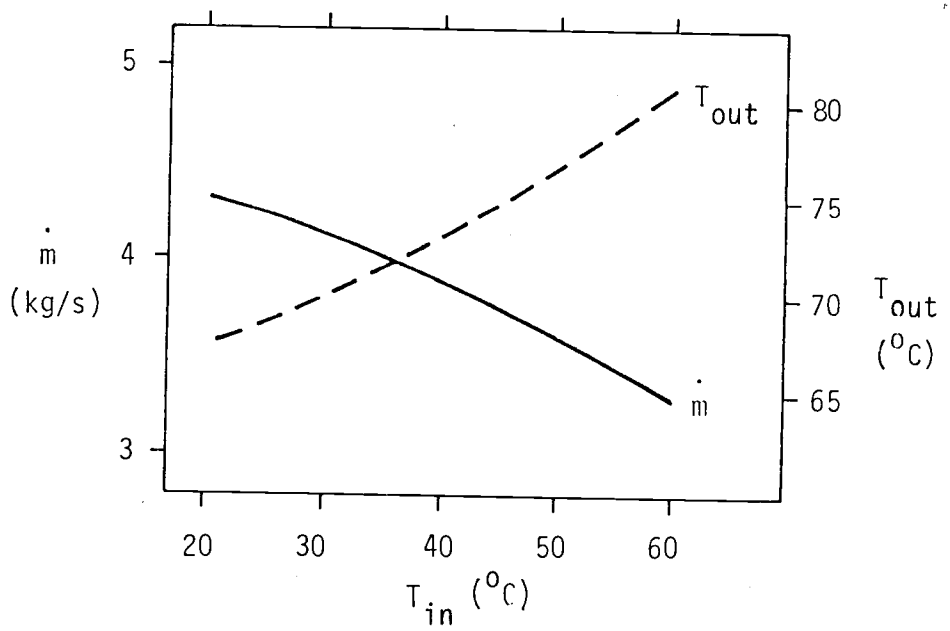

Figure 2.10. Effect of inlet temperature.

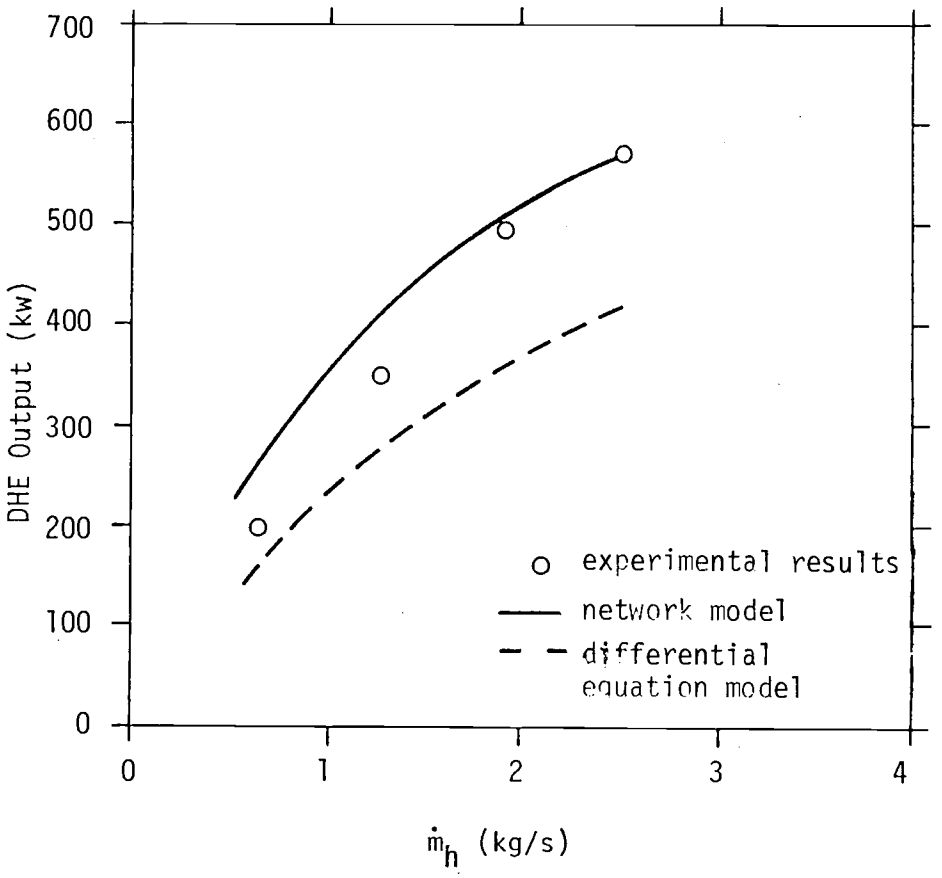

FIGURE 2.11. Comparison of model and test results.

fluid flows. These paths may be connected by heat flow paths. See Figure 2.12 for notation.

The governing equations for these networks are derived by applying conservation of mass, momentum, and energy to nodes and paths. The definition of the overall heat transfer coefficient is also used for conductive paths. There are three possible equations of motion, depending on the type of flow path being modelled. The three types are: (i) a convective loop; (ii) pressure forced conduit flow; and (iii) pressure forced porous media flow. Only the convective loop equation is used in the models presented here; the others are included for completeness. The general form of the governing equations is shown in Figure 2.13.

The models discussed below all include the following assumptions: (i) conduction is negligible except through the casing and into the DHE; (ii) the source temperature is known; (iii) the source mass flow rate is unrestricted; (iv) fluid properties are constant except for density changes in the convective motion equation; (v) temperature differences are assumed small; and (vi) constant heat transfer coefficients. The last assumption restricts the model validity to small changes in mass flow rate through the casing.

The network model corresponding to the differential equation model for the cased well with DHE previously discussed is shown in Figure 2.14. The thermal output of the DHE is Q, T_{out} is the outlet temperature and HR_{21} is the heat transfer through the casing. W_1 and W_2 relate the mass flow rate to the average temperature difference. Other symbols are as previously used. T_2 is assumed

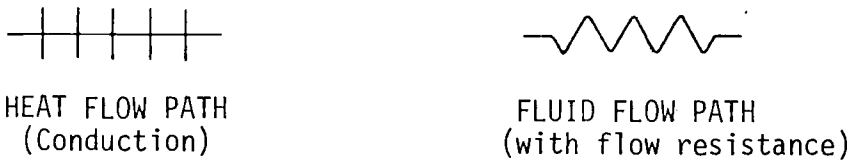

FIGURE 2.12. Graphical notation for network models.

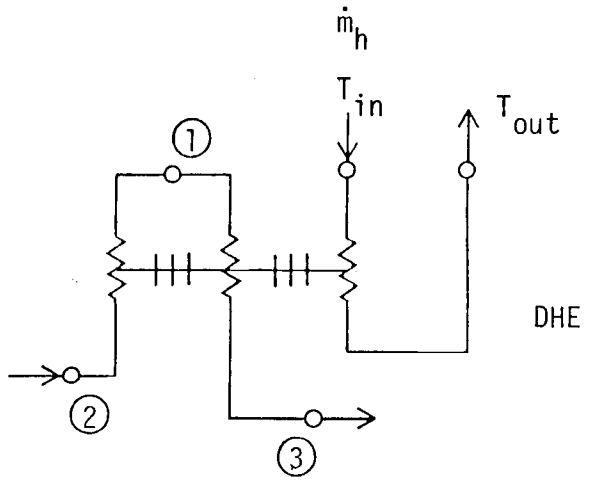

FIGURE 2.14. Network model with DHE.

Conservation of Mass:

$$\dot{m}_{ij} = S_i$$

where $\dot{m}_{ij}$ = mass flow rate from node i to node j.

S_i = source strength at node i

Motion:

$$(w_1+w_2)\dot{m}^2 = \Delta T_{avg} \qquad \text{Convection}$$

$$\dot{m}_{ij}^2 = C_{ij}(P_i-P_j) \qquad \text{Conduit Flow}$$

$$\dot{m}_{ij} = C_{ij}(P_i-P_j) \qquad \text{Porous Media Flow}$$

where

$$w_1 = \frac{2f_{fi}}{\rho^2 g A_i^2 De_i \beta}$$

$$w_2 = \frac{2f_{fo}}{\rho^2 g A_o^2 De_o \beta}$$

C_{ij} = constants of proportionality

ΔT_{avg} = average temperature difference between sides of convection loop

Energy:

$$\sum_j \dot{m}_{ij} T_j = \sum_j \frac{HR_{ij}}{C_p} + S_i T_i$$

Figure 2.13. General Form of Governing Equations.

to be at T_b, the source temperature. The governing equations are:

Convective motion: $$2(w_1 + w_2)\dot{m}^2 = T_2 - T_3 \tag{12}$$

Energy: $$T_2 - T_3 = Q/C_p\dot{m} \tag{13}$$

$$T_1 - T_3 = Q/C_p\dot{m} + HR_{21}/C_p\dot{m} \tag{14}$$

where

$$HR_{21} = \frac{U_i A_c}{2}(T_2 - T_3) \tag{15}$$

$$Q = \dot{m}_h C_p (T_{out} - T_{in}) \tag{16}$$

$$w_1 = \frac{2f_{fi}}{\rho^2 g A_i^2 De_i \beta} \tag{17}$$

$$w_2 = \frac{2f_{fo}}{\rho^2 g A_o^2 De_o \beta} \tag{18}$$

$$Q = \frac{U_h A}{2}(T_1 + T_3 - T_{in} - T_{out}) \tag{19}$$

Combining these equations to give a single equation for $\dot{m}$ gives:

$$\left[\frac{2C_p}{UA} + \frac{1}{\dot{m}_h}\right]\dot{m}^3 + \dot{m}^2 + \frac{U_i A_c}{2C_p}\dot{m} - \frac{T_b - T_{in}}{w_1 + w_2} = 0 \tag{20}$$

After $\dot{m}$ is obtained from this equation, the other unknowns are determined by:

$$Q = 2C_p(w_1 + w_2)\dot{m}^2$$

$$T_{out} = T_{in} + Q/\dot{m}_h C_p$$

$$T_3 = T_2 - Q/C_p\dot{m}$$

$$T_1 = T_2 - \frac{U_i A_c}{2\dot{m}^2 C_p^2} Q$$

These equations allow a relatively simple investigation of the effects of varying parameters. Shown in Figure 2.15 are the results of this model for various combinations of length and casing diameter. The conclusions reached with the differential equation model are confirmed by the network model. Although the quantities differ somewhat, the effect of changes in length and casing diameter is the same. The figure shows that proper sizing of the casing is even more important as the length becomes greater. Not shown on the diagram is that maximum output occurs with D_i approximately .16 m.

Until this point the effect of mixing at the bottom of the well has been ignored. Perforations at the bottom of the well allow part of the field from inside the casing to mix with fluid outside the casing and be recirculated up the outside of the casing. No provision is made for this occurrence in the previously discussed models. The following model provides a means of estimating the effect of this mixing on the mass flow rate through the casing and on DHE output.

The mixing model considered is shown in Figure 2.16. In this model the temperature at node 2 (T_2) is no longer fixed at $T_2=T_b$ but is determined by the mixing of flow from the source and recirculated fluid. The flow rate of the source is S and

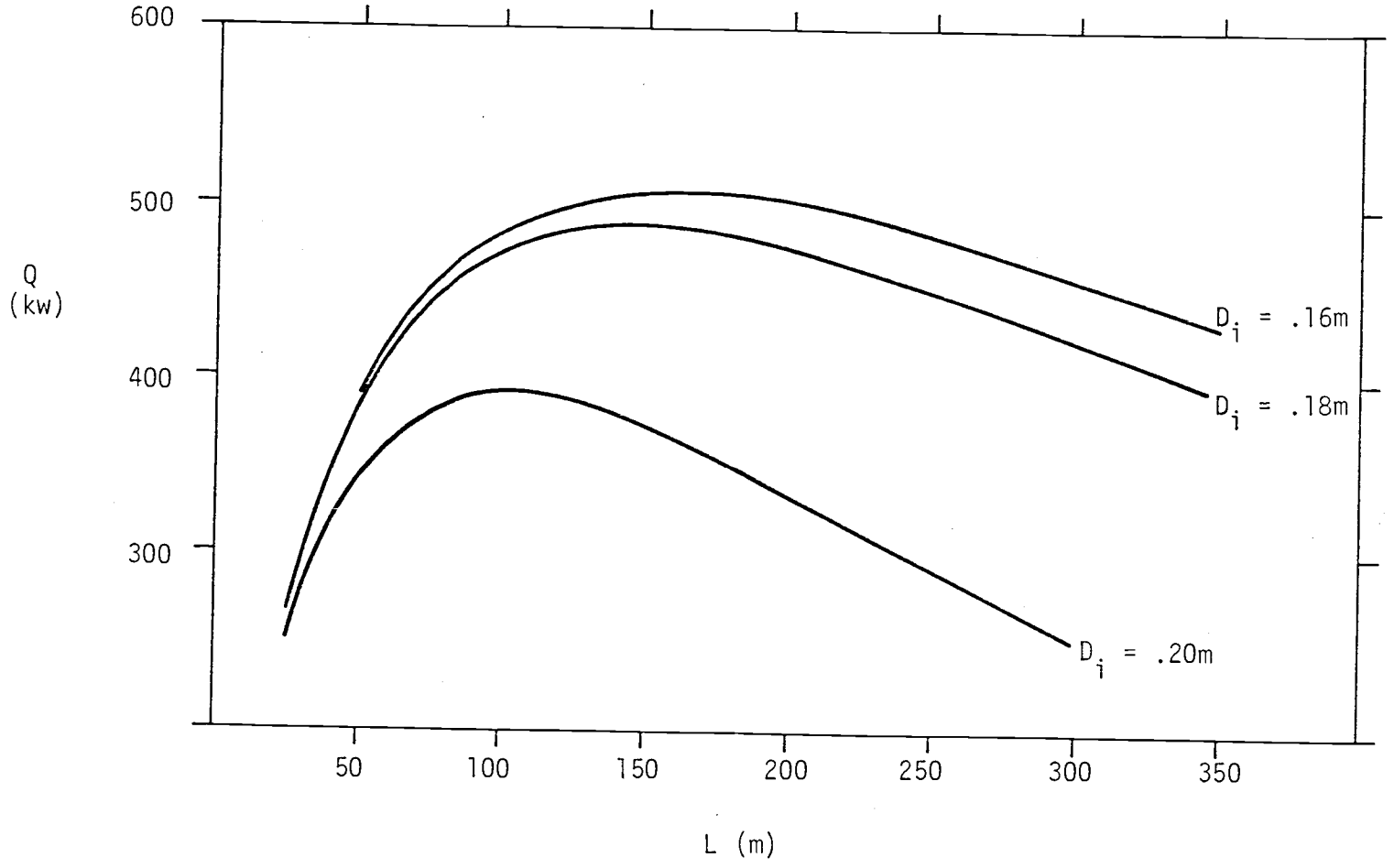

Figure 2.15. Effect of length and casing diameter on output.

$\dot{m}$ = 2.5 kg/s, T_{in} = 50°C, D_h = .0508m

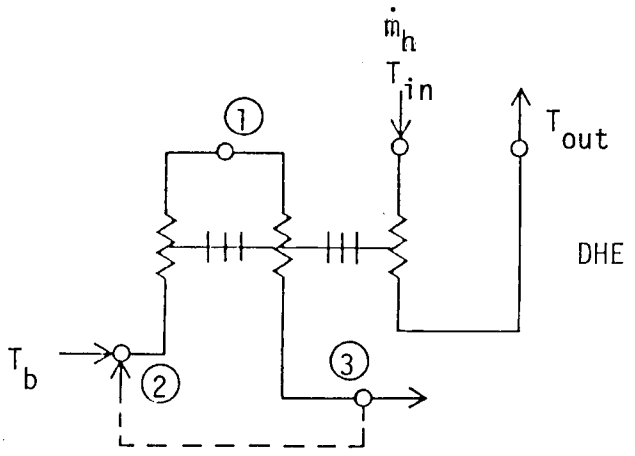

FIGURE 2.16. Network Model with Recirculation.

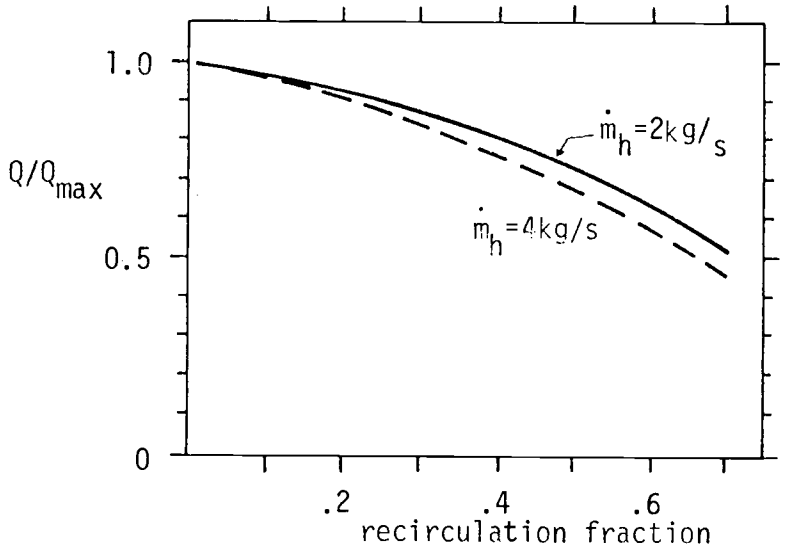

FIGURE 2.17. Results of recirculation model.

the fraction of flow through the casing that is recirculated is r. Other parameters are as previously indicated.

The governing equations then consist of previous equations (12) - (19) and the following:

Mass conservation: $S + k\dot{m} = \dot{m}$

Energy: $T_2 = rT_3 + (1-r)T_b$

If this system of equations is reduced to an equation for the single unknown $\dot{m}$, the following equation results:

$$\left[\frac{2C_p}{UA} + \frac{1}{\dot{m}_h}\right]\dot{m}^3 + \frac{1+r}{1-r}\dot{m}^2 + \frac{U_c A_c}{2C_p}\dot{m} - \frac{T_s - T_{in}}{w_1+w_2} = 0 \quad (21)$$

where the terms are as previously defined. When equation (21) is solved for $\dot{m}$, the other unknowns can be determined from the following:

$$Q = 2C_p(w_1+w_2)\dot{m}^3$$

$$T_{out} = T_{in} + Q/\dot{m}_h C_p$$

$$T_2 = T_s - (Q/\dot{m}\, C_p)\left(\frac{r}{1-r}\right)$$

$$T_3 = T_2 - Q/\dot{m}\, C_p$$

$$T_1 = T_2 - \frac{U_1 A_c}{2C_p\dot{m}}(T_2 - T_3)$$

Some results of this calculation are shown in Figure 2.17. The graph shows that moderate recirculation and energy extraction rates do not have a large effect on energy output. When greater amounts of energy are withdrawn, the recirculated fluid becomes increasingly colder and its effect becomes somewhat greater.

2.4 Increasing DHE Output

Downhole heat exchanger output can be increased by three basic methods: (i) increased film coefficients; (ii) increased heat transfer area; and (iii) increased log mean temperature difference (LMTD).

The film coefficient can be increased by increasing the flow velocity and installing turbulence promoting devices. The flow velocity can be increased by the following methods: (i) proper sizing of the casing and wellbore to provide a low resistance path for the flow of liquid up the outside of the casing; (ii) slots of adequate size; and (iii) pumping fluid past the DHE. Turbulence promoting devices have the unfortunate effect of increasing friction which tends to decrease the velocity since the flow is due to thermosyphoning only and is therefore sensitive to flow resistance.

The importance of making the outer annulus sufficiently large when the DHE consists of a single loop is very evident from Figure 2.8 and Figure 2.15, which show that the DHE output is very sensitive to the casing diameter. When multiple loops are present, the output becomes less sensitive to casing diameter and the optimum diameter is larger than when only a single loop is present. The optimum diameter for the casing becomes smaller as the distance between perforations increases.

Pumping fluid past the DHE appears to add considerable complication and expense, and was therefore not considered in this work.

Area can be increased by: (i) adding more tubing to the heat exchanger; (ii) using multiple small diameter tubes; (iii) adding fins;

and (iv) providing a high conductivity path from the heat exchanger to the casing to use the casing as a fin. Fins are attractive if there is a significant difference in the film coefficients between the inside and outside of the heat exchanger tubes. Fins are added to the outside of the heat exchanger tubes, which is the side with the lower heat transfer coefficient. If the heat transfer coefficients are approximately equal, the gain from fins is slight and additional area of plain tubing is generally the most economical method of increasing the area. Multiple small tubes have a greater surface area than the same capacity using a large tube, but would be somewhat more expensive and difficult to install.

An interesting but rather impractical method of increasing the surface area is to have a good thermal connection between the casing and the DHE so that the casing functions as a large fin for the DHE. This could be very effective but would make installation and replacement of the DHE very difficult.

Figure 2.18 shows the effect of adding fins to the DHE. It is evident from Figure 2.18a that with a mass flow rate through the DHE of 2 kg/s, approximately the rate measured for thermosyphoning DHEs (Culver et al., 1974), there is only a small increase in output possible, as the fluid in the DHE is already heated nearly to the maximum possible temperature.

With a higher flow rate through the well, Figure 2.18b shows a significant improvement for a finned DHE. An increase of about 40% is indicated by the network model. The model shows 24 fins about .0127m by .0064m to be optimal for the well dimensions indicated.

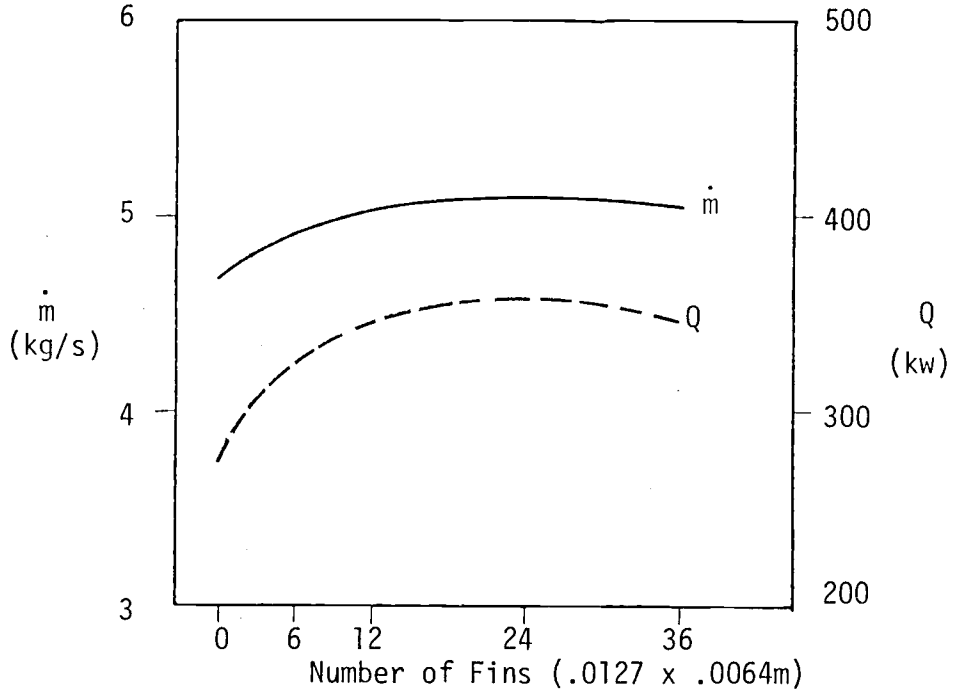

FIGURE 2.18a. Effect of Fins on model results.
$\dot{m}_h$ = 2kg/s T_{in} = 50°C (Network model)

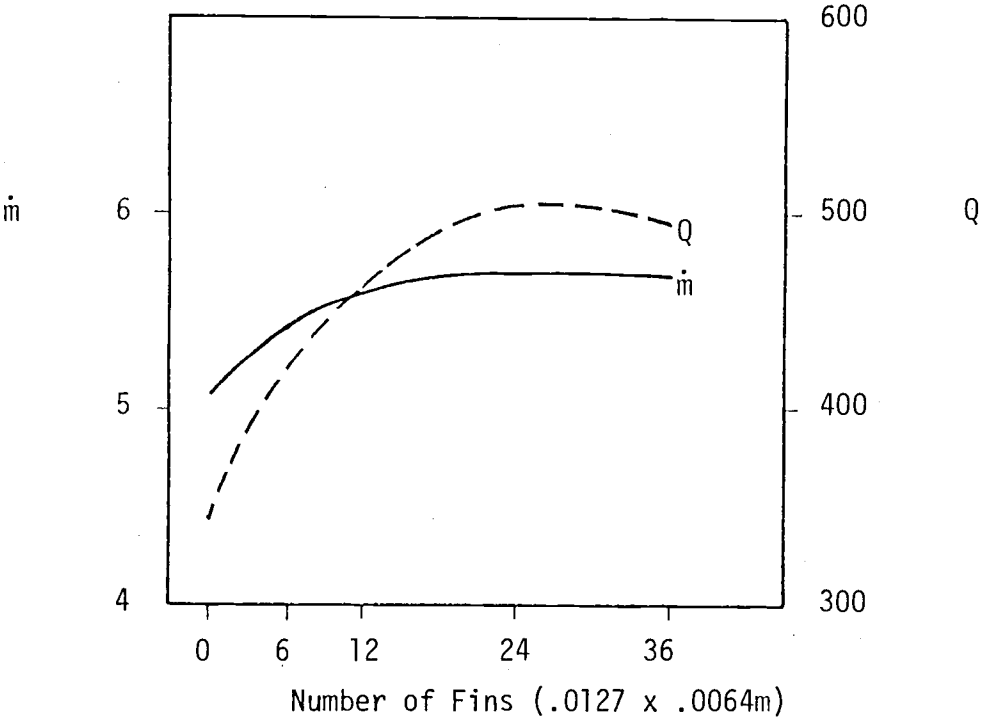

FIGURE 2.18b. Effect of fins on model results.
$\dot{m}_h$ = 4kg/s T_{in} = 50°C L=40m
(network model)

The use of multiple small diameter tubes can result in significantly higher output than a finned tube, as shown in Figure 2.19. For a mass flow rate of 4 kg/s, the network model with 12 loops of .0254m pipe results in an increase in output of approximately 100%. Increasing the number of loops beyond 12 resulted in decreased output. While fins can significantly increase output, multiple loops are necessary for really large increases. These results are for flow in parallel loops and with friction factors and heat transfer coefficients assumed constant. The effect of allowing the friction factors and heat transfer coefficients to vary results in a decrease in the optimum number of tubes and fins.

The log mean temperature difference (LMTD) depends on the direction of flow in the well. If flow is down inside the casing, the hottest point will be at the top. If there is free thermosyphoning with little mixing at the well bottom, the ideal arrangement is to have the fluid taken quickly to the well bottom. Then, after it has been warmed, give it a final heating at the top before leaving the well. This arrangement is not particularly attractive, however, since caving may occur. If appreciable caving does occur, thereby blocking the outer annulus, this method will be considerably inferior to having additional area at the well bottom where it would be more accessible to the hot fluid flowing in the aquifer.

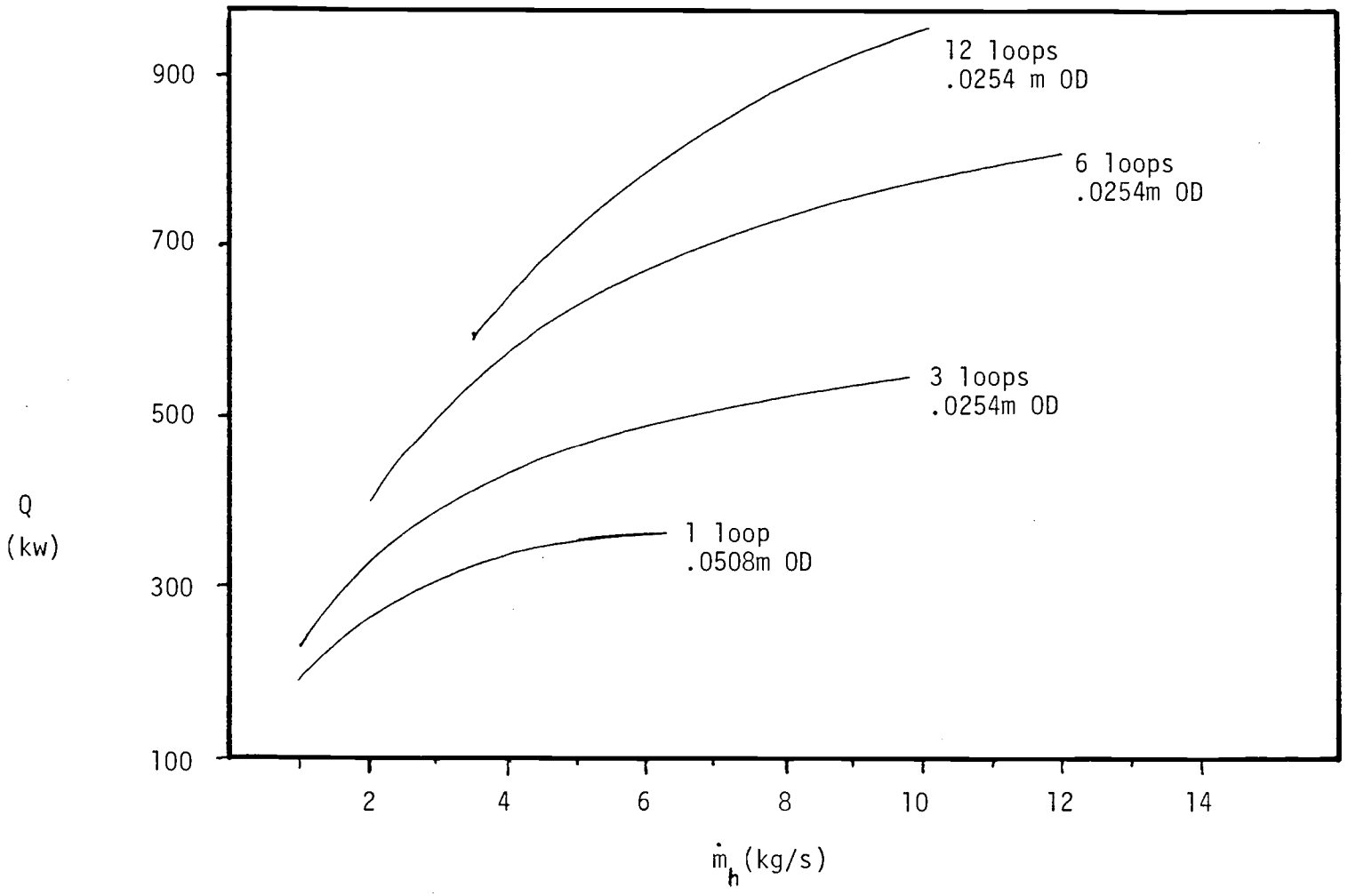

Figure 2.19. Effect of multiple tubes on model results. (Network model)
L = 40m D_c = .203m

3. CORROSION AND SCALING

Consideration of corrosion and scaling is important to the success of a DHE because:(i) the cost of replacement of a corroded DHE;and (ii) the reduction of thermal output from a DHE caused by scale and corrosion products. Figure 3.1 shows a photograph of several DHE pipes that have been removed from a geothermal well after failure. Scale and corrosion products cover much of the surface and the pipe wall has been perforated.

This chapter considers the corrosion and scaling of the DHE. Since the fluid inside the DHE itself is in a closed system, scaling and corrosion can be controlled by the usual methods for closed systems such as hot water heating systems. Thus the corrosion and scaling problems to be addressed here concern the outside of the DHE which is exposed to the geothermal fluid. The specific composition of the geothermal fluid strongly influences both scaling and corrosion. Consequently the several topics covered here include:(i) composition of the geothermal fluid; (ii) scaling; (iii) aqueous corrosion; and (iv) corrosion control methods.

3.1 Composition of Geothermal Fluid

Marshall and Braithwaite (1973) list common impurities in geothermal fluids as: silica, chloride, fluoride, borate, sulphate, carbonate, sodium potassium, lithium, calcium, magnesium, hydrogen sulphide, carbon dioxide, and hydrogen chloride. The significant impurities at Klamath Falls are: carbonate, sodium, potassium, silica, and

Figure 3.1. Photograph of DHE pipe.

Table 3.1 Composition of Water and Corrosion Rates

System	Reykjahlío	Reykir	Bolholt	Seltjarnarnes	Húsavík	Hvammstangi	Mógilsá
Temperature at testing site, °C	98	96	83	84	80	80	70
Corrosion rate µm/year	2.8	0.7	1.0	0.6	1.2	4.8	40
Max. pitting depth µm/year	60	50	50	0	120	105	510
pH	9.75	9.70	9.55	8.50	9.55	9.45	8.05
Oxygen (O_2), ppm	0.0	0.0	0.0	0.0	0.0	0.0	0.0
Silica (SiO_2), ppm	91	74	128	117	186	98	124
Calcium (Ca^{++}), ppm	2.0	2.8	2.4	105	9.1	27.8	10.6
Sodium (Na^{+}), ppm	46.4	44.0	53.6	337	47.0	160	81.0
Magnesium (Mg^{++}), ppm	<0.1	<0.1	0.0	0.2	0.0	0.0	0.1
Chloride (Cl^{-}), ppm	14.3	15.2	27.2	528	10.1	141	28.5
Sulphate (SO_4^{--}), ppm	20.2	15.0	17.1	180	27.8	137	50.2
Bicarbonate, (HCO_3^{-}), ppm	30.0	30.0	27.0	20.0	46.0	17.0	130
Carbonate (CO_3^{--}), ppm	11.0	10.0	7.0	0.6	9.6	3.0	0.9
Dissolved solids, ppm	228	194	280		336	617	367

Data from Lindal (1974) and Lund et al. (1976)

Table 3.1 Continued

System	Selfoss	Dalvik	A of GC KF	Wendling KF	Crane KF	Thexton KF
Temperature at testing site, °C	82	55	90	94	75	73
Corrosion rate µm/year (waterline/below)	16	55	236/7.6	/7.6	/6.6	/19
Max. pitting depth µm/year	320	275	914(WL)			100
pH	8.75	10.25	7.80	8.06	8.3	8.0
Oxygen (O_2), ppm	<0.1	1.2	2.60	3.1	2.0	1.4
Silica ($S.O_2$), ppm	69	90	111	119	90	93
Calcium (Ca^{++}), ppm	25.5	4.5	30	36	28	32
Sodium (NO^{+}), ppm	170	42.0	212	231	180	207
Magnesium (Mg^{++}), ppm	0.1	0.0	.2	.2	0	0
Chloride (CI^{-}), ppm	245	8.8	55	61	47	55
Sulphate (SO_4^{--}), ppm	51.4	13.8	402	484	370	408
Bicarbonate, (HCO_3^{-}), ppm	40.0	13.7	56	51	48	53
Carbonate (CO_3^{--}), ppm	1.0	13.7	0	0	.6	0
Dissolved solids, ppm	603	224				

chloride. Culver, Lund and Svanevik (1974) found geothermal water from Klamath Falls wells characterized by low total alkalinities (40 mg $CaCO_3$), silica typically 70-90 mg/l, Langlier saturation index in the range +.02 to +.75, and sulphate the principal negative ion on a mass basis. There is a significant variation from well to well, however.

Composition of the water in some Klamath Falls geothermal wells is compared to water from geothermal wells in Iceland in Table 3.1, which also compares the corrosion rates of mild steel in the wells (discussed later). Carbonate is particularly important because of its influence on scaling and the large influence of carbonate scale on corrosion. Sulphate and chloride concentrations are very important in determining corrosion rates.

3.2 Scaling

High temperature geothermal systems often have severe scaling problems. An example is the geothermal brine in the Salton sea area of California which contains 25 percent solids and can plug a pipe in a matter of days (Owen, 1976). Scaling problems in low temperature systems such as Klamath Falls are generally much less severe.

Scale in both types of systems is composed primarily of silica and calcium carbonate (Lindal, 1974), though silica is much less important in the low temperature systems. The rate of scale formation (precipitation) is a function of temperature, concentration, pH, solubility and the nature of the surface.

Scaling and corrosion are interdependent. The scaling rate is dependent on factors which are influenced by corrosion: Lindal (1974) states that the corrosion products of copper and steel, and coatings of zinc, tend to increase the deposition rate of silica. The corrosion rate is greatly affected by a layer of scale coating the surface: if the coating is thin, dense, adherent and complete, the corrosion rate will be greatly reduced. If the scale tends to be patchy, pitting is likely due to differential aeration (discussed in Section 3.3). The corrosion rate of mild steel in water is greatly reduced by the formation of a thin adherent layer of calcium carbonate scale and this is the reason why soft waters tend to be much more aggressive than hard waters.

Prediction of Scaling

The amount of information on scaling in the literature that is directly relevant to DHEs is rather limited. Most of that available is concerned with boilers which have rather different operating conditions than those in geothermal wells. The DHE is heated by the surrounding fluid and hence is colder than the fluid, whereas in a boiler, the tubes are warmer than the fluid.

A widely used indicator of the scale forming tendencies of natural waters is the Langlier saturation index (Langlier, 1936). This index shows the tendency for water to form calcium carbonate scale by denoting how close the water is to saturation with respect to calcium carbonate. A negative value of the Langlier saturation index indicates a tendency to dissolve scale and a positive value indicates a tendency

to deposit scale. A value of about +.5 is considered most desirable to minimize corrosion. For very large positive values scale tends to be a problem and the scale tends to be less adherent. The Langlier saturation index is not always accurate in predicting corrosive tendencies of waters, since certain ions can cause the carbonate scale to lose its protective properties and result in pitting. Lime and sodium carbonate are often added to closed systems to adjust the Langlier saturation index to the desired value.

Attempts are underway to find analytical and empirical equations that more completely describe fouling behavior. A general program of this type is that at HTRI (Taborek, Aoki, Ritter, Palen and Knudsen, 1972). Several models for the scaling rate, generally of the form: scaling rate equals deposition rate minus removal rate, have been proposed, but all require many experimentally determined parameters and so are of limited use in this study. The goal of a project underway at Battelle Northwest is to develop a computer model to predict scaling rates as a function of time as part of a large project related to geothermal electricity generation (Shannon, Walter and Lessor, 1976). Experimental studies to provide the necessary data are included. If the model is successful and is general enough to be applicable to low temperature systems as well as high temperature systems, it could be a very useful tool in further analysis of scaling problems at Klamath Falls.

Scaling Control

Scaling can be controlled by changing the environment. This is

very effective in closed systems, but is difficult in an open system such as a geothermal well. The substrate has an effect on scaling, but only during the initial stages since once a film of scale has formed all the solution sees is scale surface regardless of what surface is under neath. A substrate such as teflon will tend to reduce scale buildup, but even teflon is not immune to scaling.

The flexibility of certain materials tends to break up the brittle layer of scale. This can be accomplished by using flexible tubes of plastic for DHE tubes, or by allowing differential expansion of a metal heat exchanger tube to loosen some scale. This occurs to some extent with low fin heat exchanger tubes (Kern and Kraus, 1972).

It seems that a nucleation process is important in some types of scaling. Taborek et al. (1972) found that incompletely cleaned material fouls much more rapidly than thoroughly cleaned material.

The most effective method of controlling scale is to mechanically remove the scale. Other methods, such as electrolytic descaling (Cook, et al., 1954) and cavitation (Thiruvengadam, 1976) have been proposed, but are experimental at this time.

The most effective means of scale control is mechanical removal of the scale. Since this involves removing the DHE, cleaning it and replacing it, there would be a great deal of labor involved. The evidence of scaling that I've seen is not severe enough to warrant such measures. The other control techniques, such as relying on differential expansion, would only partially help the situation, and do not seem to be very economic alternatives. Corrosion control should influence a

beneficial effect on scale, and cathodic protection tends to cause some descaling (Cook et al., 1954), and this seems to be all that is warranted with present information.

3.3 Aqueous Corrosion

The waterline was found to be the most aggressive environment in the wells in corrosion tests (Lund et al., 1976) and failure of DHEs occurs most commonly at the waterline (Culver et al., 1974). Corrosion consists of both general rusting and localized corrosion which leads to leaks in the DHE that eventually render it unusable. Stray current corrosion is also believed to be a factor in the failure of DHEs at the bottom of the loop (Newcombe, 1976).

The most common method of corrosion control is to pour a small amount of paraffin or used motor oil into the well (Lund et al., 1976). This apparently coats the pipe near the waterline and provides a barrier for oxygen diffusion into the water. The effectiveness of this procedure is unknown.

It is not surprising that corrosion occurs in these wells, since most metals are thermodynamically unstable in a geothermal well environment, as indicated by the negative change in Gibbs free energy between the metal and its compounds with elements found in the environment. Thermodynamic instability alone, however, does not make a material unfit for use: the reaction rate is of overwhelming importance. The mechanism of aqueous corrosion is electrochemical in nature and an understanding of this basic mechanism is fundamental for

predicting of corrosion rates and understanding corrosion control methods.

Electrochemistry

Four things are necessary for corrosion to occur by an electrochemical process: (i) an anode;(ii) a cathode;(iii) an electrolyte; and (iv) an electrical connection between anode and cathode. The anode is where oxidation of the metal takes place and the metal is corroded away. At the cathode, reduction takes place. Although no metal is corroded away at the cathode, it is still of great importance in corrosion control methods. During corrosion the rate of oxidation at the anode must equal the rate of reduction at the cathode (otherwise the metal would become spontaneously charged). Since these two rates must be equal, the rate can be controlled at both anode and cathode. The electrolyte in the well consists of water containing various impurities. The metal itself usually furnishes the necessary electrical connection between anode and cathode.

Uhlig (1963) lists three main types of electrochemical cells responsible for corrosion in an aqueous environment:

1. Cells with electrodes of different materials, such as two types of metals, different alloys or phases, impurities, and even different amounts of cold work. When placed in contact with an electrolyte these different materials exhibit a potential difference and corrosion will occur at the anode if current is allowed to flow.

2. Cells which have identical electrodes, but each electrode is in contact with a different solution.

3. Cells whose electrodes are at different temperatures can also exhibit a potential difference and result in corrosion. To these I add another:

4. Cells due to an externally impressed voltage.

In general, corrosion will be the result of a combination of two or more of the above types of cells.

Types of Corrosion

These cells occur in many different forms. Particular manifestations of corrosion can be grouped into the following categories:

(1) Uniform corrosion, in which the surface corrodes at essentially the same rate all over. This is thought to be due to microscopic cells arising from impurities, grain boundaries, different crystal orientations, etc.

(2) Pitting is the result of severe local corrosion, leading to deep pits and penetration of the metal. There is an autocatalytic effect as the pit deepens and provides protection from the surrounding environment for the accumulating ions resulting from corrosion. A type of pitting common in DHEs is tuberculation, in which the corrosion products form a shell over the deepening pit. This protects the inside of the pit from the environment and allows local conditions of pH and concentration in the pit to develop that differ substantially from the conditions outside the tubercule.

Pitting is also related to area effects. A large cathode coupled to a small anode can lead to severe localized corrosion at the anode.

This is an important consideration with coatings for corrosion protection, since few coatings are perfect. A few small holes in a coating over an anode can lead to rapid pitting when coupled to a large cathode.

Halide ions, especially chloride ions, break down or prevent passivity in iron and stainless steels. Breakdown occurs locally rather than over the entire surface. The result is a small anodic area surrounded by a large cathodic area. The combination is known as a "passive-active cell" and it leads to severe pitting.

(3) Crevice corrosion is related to pitting, but begins with a crevice such as that formed between two parts bolted or riveted together. The resulting crevice forms a pocket which is partially shielded from the external environment. This can result in changes in the local environment (in the crevice) sufficient to result in severe local corrosion, deepening the crevice with the same autocatalytic effect found in pitting.

A major cause of this type of corrosion is differential aeration, which was discovered by Evans in 1923 (Evans, 1960). The oxygen concentration in contact with a metal varies from one location to another. Inside the crevice the oxygen concentration will be lower than outside. The differing local environments are sufficient to set up a corrosion cell capable of producing severe corrosion in the deaerated region which is the anode. The difference in chloride concentration between the interior of the crevice and outside the crevice is also an important factor in crevice corrosion.

(4) Stray Current Corrosion is due to externally applied currents,

such as those due to power plants, welders, cathodic protection systems, or other sources of current. These stray currents cause corrosion where they leave a metallic structure and may be of great importance in the early failure of some DHEs. Ewing (1948) states that direct current causes much more damage than alternating current.

The amount of metal corroded can be approximately calculated by Faraday's law. Iron, for example, will be corroded at the rate of 9.1 kg per year for a current of one ampere. The accuracy of the calculation decreases for very large and very small currents because other mechanisms become important.

(5) Other types of corrosion, which will be discussed only briefly because they are unlikely to be important in the corrosion of DHEs, are: (i) intergranular corrosion, in which the corrosion takes place between grains of metal in the grain boundary causing the metal to fall apart; (ii) erosion corrosion, in which erosive action combines with corrosion to produce much larger metal losses than either corrosion or erosion alone would be expected to produce; (iii) selective leaching, in which some components of an alloy are leached away leaving a sponge-like mass of the remaining components behind; and (iv) stress corrosion, in which the combination of stress and a corrosive environment results in catastrophic failure at stresses far below those usually necessary for catastrophic failure and with little or no visible evidence of corrosion. Stress corrosion is primarily a problem with high-strength alloys.

Pourbaix diagram

Many factors are involved in determining the severity of corrosion. A Pourbaix diagram, as shown in Figure 3.2, can be very useful for examining corrosion behavior (Pourbaix, 1974). This diagram shows the conditions of electrode potential and pH for which iron (in water at 25°C) is:(i) thermodynamically stable (immunity); (ii) protected by an insoluble adherent layer of corrosion products (passive); and (iii) corroded. The diagram is completely accurate only for water of a specific composition under specified conditions, but it will help to show the influence that pH and electrode potential have on corrosion.

Lines a and b on the diagram show the limits of thermodynamic stability for water. Outside these limits water can decompose into hydrogen and oxygen. In water and nonoxidizing solutions, iron will corrode with the evolution of hydrogen. This reaction will be most vigorous in acid and will nearly stop between pH 10-13. In this pH range the iron is covered by a thin layer of oxide. This layer of oxide controls corrosion of the iron by controlling the diffusion of oxygen to the iron surface. The process of protection by a layer of corrosion product is known as passivation. Many metals owe their usefulness to passivation.

The electrode potential of iron increases in the presence of oxidizing agents, including oxygen, depending on the particular reactions involved. The diagram indicates that this can tend to passivate the metal or increase the corrosion rate, depending on the pH - potential region considered. Passivation will be much easier when the corrosion

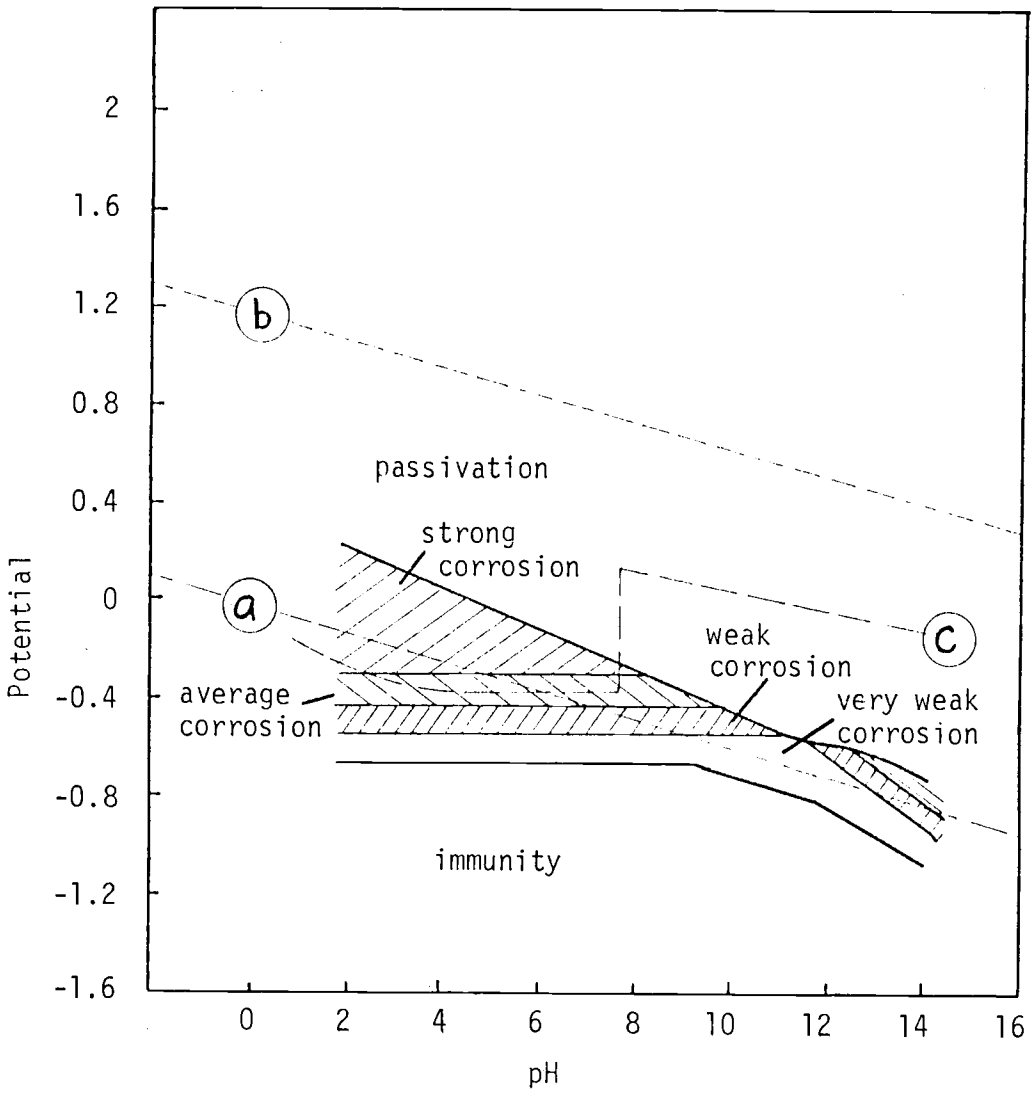

Figure 3.2. Pourbaix diagram for iron at 25°C. (Pourbaix,1974)

range of potential is small, such as for pH 10-12. Below a pH of 8 passivation will be difficult or impossible. For this reason closed systems are often buffered to a pH of 10-12.

The presence of oxygen will shift the line a to position c so that in the pH range 7-10 a current flowing between an aerated region and a nonaerated region will tend to passivate the aerated region and corrode the deaerated region.

Some approaches to corrosion control are also evident from the diagram (Pourbaix, 1974): (i) cathodic protection, which lowers the potential of the metal into the immunity region; (ii) anodic protection or protection by passivation, which encourages the growth of a protective film on the metal; and (iii) protection by alkalinization, which changes the pH into the region where the metal is easily passivated, pH 10-13. Cathodic protection is a promising method of corrosion control in DHEs and will be discussed in detail later.

Polarization

A key concept in determining corrosion rates is polarization. Polarization is the difference in electrode potential between current and no current conditions. It has a very large effect on corrosion rates.

Uhlig (1963) lists two types of polarization: (i) concentration polarization, which is due to changing the activity of the surface ions,

resulting in a change in potential as shown by the Nernst equation* (ii) activation polarization, which is caused by a slow electrode reaction. An important example of activation polarization is hydrogen reduction at the cathode, $H^+ = \frac{1}{2}H_2 - e^-$. The polarization introduced by this reaction is known as hydrogen overvoltage, and it is often the corrosion rate controlling factor for metals in deaerated water and nonoxidizing acids.

Figure 3.3 shows some polarization diagrams, where ϕ_a and ϕ_c are the open-circuit potentials of the anode and cathode respectively. Increasing polarization decreases the current and hence the corrosion rate.

Corrosion is said to be anodically controlled if most of the polarization occurs at the anode. The corrosion potential is then near the open circuit cathode potential.

Cathodically controlled corrosion is when most of the polarization occurs at the cathode. Iron in natural waters corrodes under cathodic control.

When electrolyte resistance is very high so that neither anode nor cathode polarizes significantly, corrosion is under resistance control. This occurs when a porous insulating coating covers a metal surface.

---

* The Nernst equation is $E=E^\circ - \frac{.059}{n} \log \frac{(a_Y)^y (a_Z)^z}{(a_W)^w (a_X)^x}$, where a_Y is the activity of Y, etc. for the hypothetical reaction

$$wW + xX - yY + zZ$$

see Mortimer (1967).

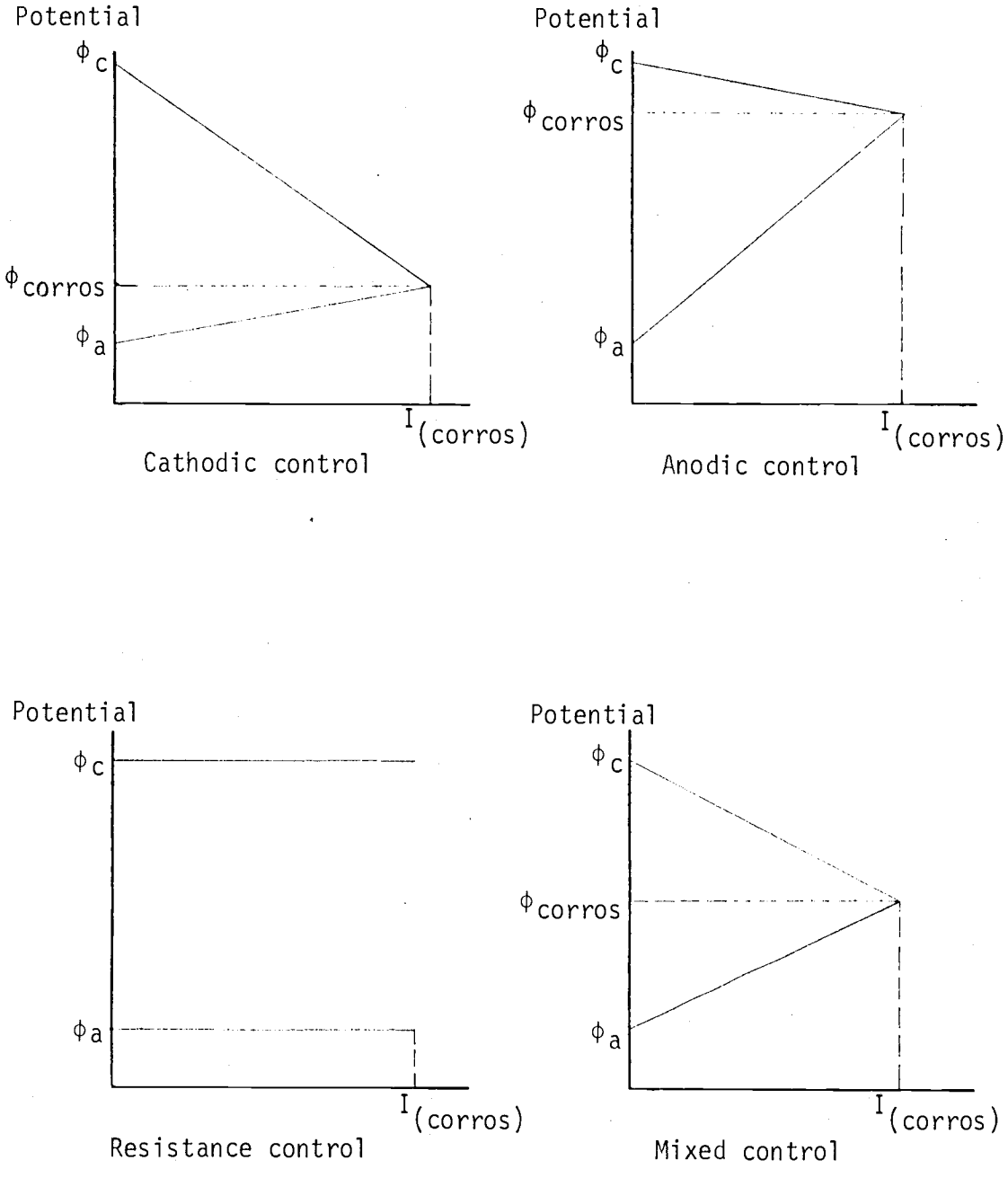

Figure 3.3. Polarization. (Uhlig, 1963)

The resistance of the electrolyte in the pores then controls the reaction rate.

When both anodic and cathodic polarization are important, corrosion is said to be under mixed control.

The extent of polarization depends very much on the area of cathode and anode. A very small anode will tend to polarize more than a large one because of the very high current densities. In addition, the diagrams in Figure 3.3 indicate total corrosion current rather than current density, so that the current density and hence corrosion rate will be locally very high if the anode is much smaller than the cathode.

3.4 CORROSION CONTROL METHODS

There are several approaches to corrosion control, including the use of a more corrosion resistant material. One can interpose some inert substance between the object to be protected and the environment. Some coatings work this way. Another method is to make the object to be protected the cathode and some cheap, easily replaced object the anode. These methods are discussed below. A fourth method is to change the environment by altering pH or concentration or by adding inhibitors to increase polarization. Inhibitors can be effective for closed systems but are rather impractical for an open system like a geothermal well and so will not be discussed in detail.

3.4.1 Material Selection

Iron and Steel

Iron and steel are of particular importance because of their low

price and availability. Mild steel is most widely used material for DHE construction.

In the range of pH 4-10, which includes the pH of geothermal waters at Klamath Falls, the corrosion rate of iron depends only on the diffusion rate of oxygen to the metal surface. The corrosion product, hydrous ferrous oxide, presents a diffusion barrier to oxygen diffusion. The presence of other films on the metal surface, such as carbonate scale, can have a major influence on the corrosion rate by presenting a diffusion barrier for the oxygen. In this pH range small variations in composition and processing of the steel make very little difference in corrosion rates in water. (This is not the case for atmospheric corrosion and corrosion in acids). However, additions which introduce galvanic effects can increase the corrosion rate in water.

Increasing the velocity of natural water tends to first increase the corrosion due to additional oxygen supplied to the surface. As the velocity increases further, sufficient oxygen may be present to partially passivate the metal.

The corrosion rate of steel in an open system increases with temperature to a maximum at about 80°C. At higher temperatures the solubility of oxygen decreases rapidly which decreases the corrosion rate.

Table 3.1 shows that corrosion rates for mild steel in geothermal wells at Klamath Falls are similar to those in Iceland.

Stainless Steel

Stainless steel gets its corrosion resistance from a thin layer of

chrome oxides on the surface. These give it very good corrosion resistance in an oxidizing environment, but it is susceptible to corrosion in reducing environments. Corrosion field tests in Klamath Falls indicate that stainless has good corrosion resistance in the geothermal wells tested, though incipient pitting and crevice corrosion were noticed on some specimens. There are two main types of stainless steel, austenitic and martensitic. Austenitic stainless steel has generally better corrosion resistance and is the type meant here by "stainless steel".

The thermal conductivity of stainless steel is about half that of mild steel, but the effect on output would be negligible compared to the effect of a coating of rust on the mild steel. A much more important consideration is that stainless steel is five to ten times as expensive as mild steel.

A possible means of corrosion control in the vicinity of the waterline is to use a section of stainless steel. This should not cause much problem with galvanic corrosion if the area of the stainless steel is small compared to the area of the mild steel, though some increased corrosion might occur at the interface of the stainless steel and the mild steel. The severity of pitting of stainless steel in the wells need to be further investigated before the use of stainless steel can be recommended unequivocally.

Copper

Copper alloys are excellent from the standpoint of thermal conductivity, but are unattractive because of a tendency toward pitting and

crevice corrosion, as shown by the OIT tests (Lund, et al., 1976). Copper generally exhibits good resistance to corrosion by natural waters but is susceptible to corrosion in the presence of sulphides, ammonia, and carbon dioxide. Sulphides may be responsible for the observed pitting. Another problem with copper is that copper ions will be deposited on other metals in contact with the solution. These ions then form local cathodes which accelerate corrosion of the other metal. This is a very serious problem with aluminum and can also be a problem with steel.

Aluminum

Aluminum pitted severely when tested in the wells by Lund, et al. (1976), but the only type of aluminum tested was a copper containing alloy (type 6061), a poor choice for an aqueous environment. Strong galvanic cells are set up with copper as the cathode and aluminum as the anode which leads to pitting of the aluminum. This effect is so strong that even running water through a copper pipe and then into an aluminum container can result in pitting of the aluminum container due to the copper ions transported by the water and deposited on the aluminum (Butler and Ison, 1966).

It is possible that a more suitable alloy (such as type 3003 or 5052) would prove serviceable, at least in wells with low chloride content. Aluminum tends to pit in the presence of chlorides. Pure aluminum has better corrosion resistance than alloys under most conditions, but is rather soft. The high thermal conductivity of aluminum would be a slight advantage.

Overall, aluminum cannot be recommended without proper testing to find alloys free of pitting problems. The greater cost of aluminum compared to steel and possible galvanic corrosion due to the steel casing are two other considerations.

Plastics

Plastics are attractive for their corrosion resistance, but other characteristics make them unattractive for use in heat exchangers. The two major problems are low thermal conductivity and loss of mechanical properties due to high temperature.

The effect of the thermal conductivity can be seen by considering the effect of a change in pipe material from steel to plastic. Using typical film coefficients from the computer model (see Appendix A) and assuming that the film coefficients are unaffected by the change in material, we find the overall heat transfer coefficient is 770 W/m^2K when made of 1/8th inch thick steel and 60 W/m^2K when made of 1/8th inch thick plastic (conductivity .2W/mK). Although this simplified analysis neglects the effect of different friction factors and a coating of rust on the steel pipe, etc., it is clear that a very substantial increase in area is required for a polymer DHE.

Aggrevating this problem is the fact that many polymers, especially the common thermoplastics, lose considerable strength when used at temperatures of 100°C. The plastic DHE would then have to be considerably thicker than the steel DHE to limit stresses and this greatly increases the problem of low thermal conductivity.

3.4.2 Control of Stray Current Corrosion

In controlling stray current corrosion the objective is to electrically isolate the DHE from the surrounding pipes so that a much greater resistance is presented to current flowing through the DHE. Increasing the resistance will decrease the current and hence corrosion. This can be done by the use of insulating couplings to connect the DHE to other pipes. Damage can also be controlled by increasing the thickness of metal at the bottom of the DHE. This serves to delay failure by stray current corrosion if it leaves through the bottom of the loop, which is said to be common (Newcombe, 1976). This would have the additional benefit of increasing the life of the DHE against failure by erosion by the water inside the DHE as it makes the 180° turn at the bottom. Cathodic protection also helps control stray current corrosion.

3.4.3 Coatings

Coatings function by three mechanisms: (i) prevent or restrict contact between the environment and the object to be protected; (ii) release inhibitive substances to decrease the rate of attack; and (iii) act as a sacrificial anode. The coatings considered here have been broken down into two categories: metallic and nonmetallic.

Metallic coatings are deposited by electroplating and other techniques and serve to prevent contact between the metal to be protected and the environment. The coating functions vary differently, though, depending on whether the coating metal is anoidc or cathodic to the base metal. If the coating is cathodic to the base metal, any small

imperfections in the coating will allow the base metal to rapidly corrode at the break, since the small exposed anode area is surrounded by a large cathode area (see discussion of pitting).

If, however, the coating is anodic to the base metal, any small defects in the coating are protected by the large surrounding area of sacrificial coating, which must corrode before the base metal. The maximum area protected by the anodic coating depends on the conductivity of the electrolyte.

Galvanized iron is iron with a sacrificial coating of zinc. This combination can be very effective, but is unsuitable for use in the geothermal wells, since at temperatures of about 80°C the relative nobility of the two metals can change so that the zinc becomes cathodic to the iron. This would lead to rapid local pitting of the steel. Corrosion test data in geothermal applications substantiate that zinc coatings are not attractive (Marshall and Braithwaite, 1973).

Cadmium is used for sacrificial coating of steel and could prove useful for protection of DHEs. Cadmium is about ten times as expensive as zinc, and so the cadmium plated steel is more expensive. The thickness of the coating is the primary factor determining the life of the coating and so a relatively thick coating is desirable. One undesirable effect of cadmium is that cadmium ions are more toxic than zinc. Testing is necessary before cadmium coatings can be recommended.

Nonmetallic coatings of interest include paints and plastic coatings. The difference is not always clear, but paints function primarily through the release of inhibitive substances as well as providing a

protective barrier, while most plastic coatings provide no inhibitive effect.

Paints have been tried on DHEs at Klamath Falls with generally poor results (Newcombe, 1976). It is not known which types of paints have been tried, but the usual linseed-tung oil paints have a lifetime measured in minutes when placed in hot water and so would not be expected to prove satisfactory. Requirements for underwater paints are very different from requirements for structural paints so that structural paint (even an anti-corrosion type) is likely to fare poorly in the wells.

Epoxy coatings have been used on mild steel in condensor systems for geothermal electricity generation and have provided adequate protection against corrosion by aerated geothermal fluids (Marshall and Braithwaite, 1973; Einarsson, 1961). Pipe (OD 3/4 through 42 inches) coated with epoxy is commercially available (Berger, 1976).

Several other organic coatings appear promising also. Phenolics have excellent resistance to hot water and can be applied in somewhat thinner coatings than epoxy (Hamner, 1970). A thinner coating is an advantage because the coating is essentially insulation over the DHE, so a thinner coating will result in less loss of thermal output from the DHE. Urethane coatings would also probably perform well in the hot geothermal water, but are less desirable because thicker coatings are necessary.

Both phenolic and urethane coatings suffer from being considerably more expensive than epoxy coatings and so epoxy coatings have the overall advantage unless phenolic or urethane coatings prove to last longer

(Hamner, 1970).

Newcombe (1976) has suggested plastic coatings as a possible cure for heat exchanger corrosion and plastic coated pipe is readily available since it is widely used for pipelines (Berger, 1976). It is possible that a thin coating of phenolic, urethane or perhaps epoxy (Hamner, 1970), especially near the waterline where the most severe corrosion generally takes place, could prove effective in controlling corrosion, but the type of coating suggested by Newcombe is unattractive for two reasons. One reason is the low thermal conductivity of the plastic coating which would greatly reduce the energy output of the heat exchanger. A polyethylene coating 40 mils thick (over a tar-like subcoating) as suggested by Newcombe would reduce the overall heat transfer coefficient for a 1/8th inch thick steel pipe from 770 W/m^2K for the bare pipe to 154 W/m^2K for the pipe with polyethylene coating. This is a very significant decrease and does not include the effect of the undercoating.

An additional problem is that the type of plastic suggested (polyethylene) is significantly affected by the temperature and would creep and distort significantly with time. Any scraping together of the DHE and the casing would tend to scrape away some of the plastic coating allowing water to get underneath it. This could lead to localized corrosion and subsequent rapid perforation of the pipe by the mechanisms previously discussed.

Use of a plastic coating over only a small area will have little effect on the output of the well but should increase the life of the DHE. It is important to choose the proper coating, however. The

coating must be capable of withstanding immersion in water at nearly boiling temperature for many years without harm. Also important is that any opening between the plastic and the steel substrate will act as a crevice and may lead to crevice corrosion, nullifying the gain from the coating. The types of coatings previously mentioned should be able to withstand the exposure to hot water, but only experiment can show whether the second problem can be successfully avoided. Even if the entire DHE is coated the problem can arise because of damage to or flaws in the coating.

3.4.4 Cathodic Protection

A properly designed cathodic protection system could virtually eliminate corrosion of DHEs and casings even in the more aggressive wells. There are two basic approaches to cathodic protection, depending on the source of the protective current. In one method an anode of a more electropositive metal is used as a sacrificial anode. In the other method the protective current is supplied by an external source, so the anode may be either some inexpensive material such as scrap iron or some special material such as platinized titanium which lasts a very long time.

The amount of protective current required from the power supply or by dissolution of the protective anode, depends on the severity of the environment. It is necessary that all parts of the object to be protected be polarized sufficiently to stop corrosion. This usually requires multiple anodes to obtain a reasonably uniform current distribution and to avoid the effect of part of the structure shielding another

part from protection. It is important that the downhole heat exchanger and the casing be electrically connected and both protected, since otherwise protection of the downhole heat exchanger alone can lead to increased corrosion of the casing. The cathodic protection system suggested by Newcombe (1976) is an excellent example of how not to design a cathodic protection system: there a diagram shows a single anode outside the casing electrically connected to the DHE. If the path of the current is traced, it becomes obvious that the interior of the casing has been made the anode in the protection circuit inside the casing, so that the DHE is protected (probably inadequately from the single anode) at the expense of the casing, a much more expensive and difficult to replace item than the DHE!

The correct procedure for complete protection of the DHE is to place multiple anodes inside the casing to obtain reasonably uniform protection of the outside of the DHE and the inside of the well casing, as shown in Figure 3.4. If desired, another anode could be added on the outside of the casing (buried in the surrounding soil) to protect the outside of the casing. Cathodic protection of the inside of the DHE requires anodes inside the DHE and is probably not practical.

The current required is important to the economics of the protection system, but is difficult to estimate accurately without field measurements. Current requirements are approximately 0.15 amp/m^2 (.015 amp/ft^2) (Applegate, 1960; Shreir, 1976) depending on the corrosiveness of the environment and other factors. If we consider a well that is 40 m below the waterline with a DHE .0508 m in diameter and a casing .203 m in diameter, the total current requirement to protect

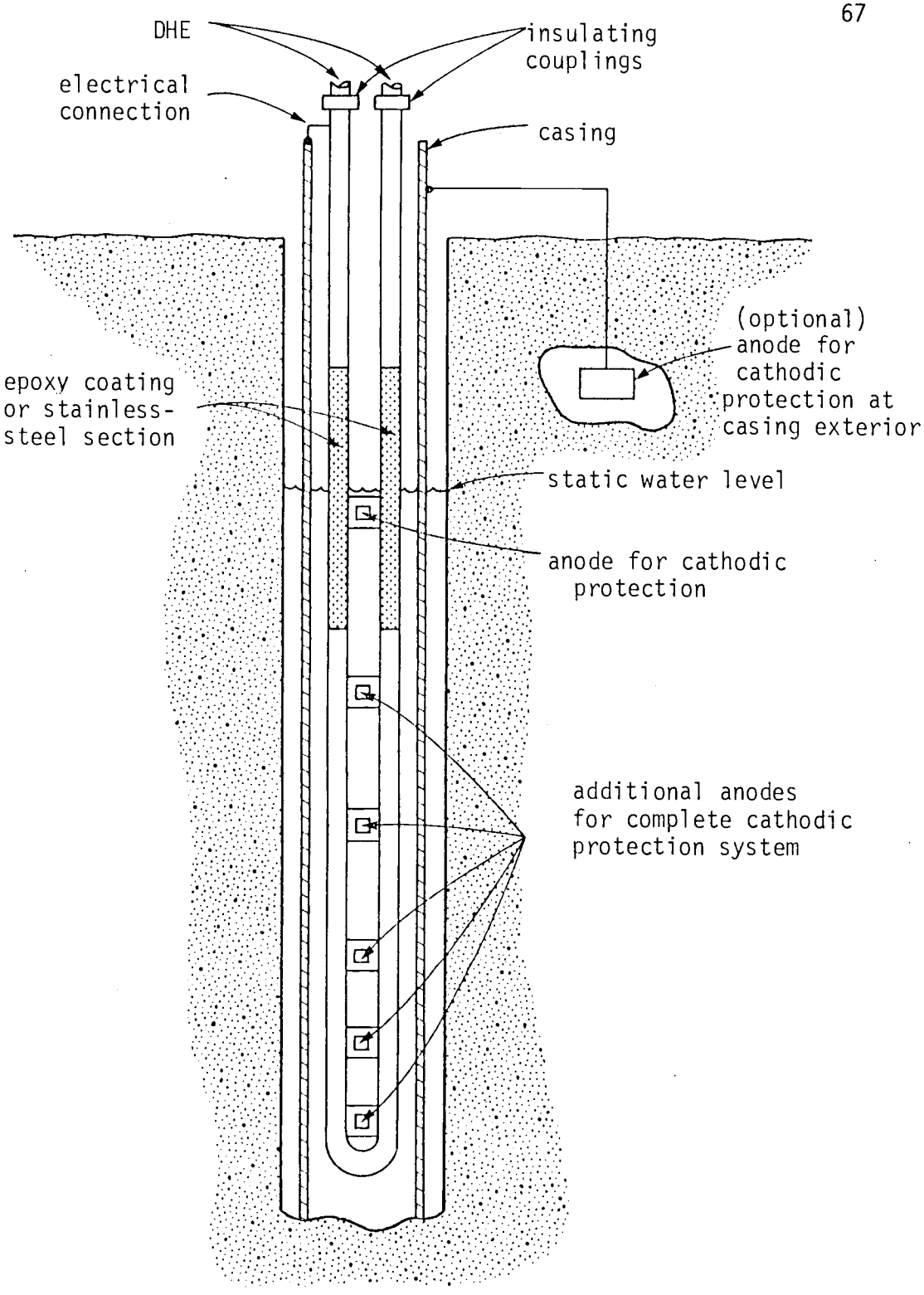

Figure 3.4. Protected well.

casing and DHE is about 18 amps at approximately 2 volts (depending on anode placement). The power requirement would then be about 20 watts or 180 kw hr/year, a minor expense compared to installation costs and the expense of replacing anodes. If a suitable insulating coating could be found, this current requirement could be reduced appreciably. Current should be kept close to the minimum value required, since current greater than the minimum required increases expense and may damage the metal or a coating. The damage is the result of changes in pH and evolved hydrogen that occur at a cathode. Mild steel is relatively insensitive to this type of damage.

A promising approach is to use a sacrificial anode attached to the DHE in the vicinity of the waterline. This should extend the life of the DHE near the waterline, though it would be effective only for that part of the DHE in contact with the water and so would be ineffective above the waterline. This would entail little additional effort and expense and a minimum of changes in procedures for installing DHEs. The protection afforded by the sacrificial anode depends on the conductivity of the water and its aggressiveness as well as the type of sacrificial anode.

There are two important considerations in the design of this local cathodic protection system. One concerns selection of the anode. Sacrificial anodes are made of three basic materials: aluminum, magnesium and zinc. Magnesium sacrificial anodes are characterized by;(i) high potential, which means increased coverage especially in environments of high resistance; and (ii) higher cost per output than the other two types. Aluminum is the most economical, but has a tendency

to passivate. Passivation of aluminum sacrificial anodes can be decreased by alloying with mercury, which is toxic, or indium. Aluminum is not suitable for use in mud and sand. Zinc is preferred for some conditions and has a higher potential than aluminum, but the reversal of the relative nobility of zinc and iron which can occur at about 80°C (as previously discussed) could make the zinc useless. The most important consideration for sacrificial anodes in the wells is the relatively high resistivity of the water, which dictates the use of magnesium anodes (Shreir, 1976).

The other consideration is stray current corrosion in the casing caused by the cathodic protection system, known as "corrosion interaction" (Shreir, 1976). This is much less a problem with sacrificial anodes than with impressed current anodes, and a good electrical connection between the DHE and the casing at the top should help eliminate the trouble.

3.5 Recommendations for Corrosion Control

Corrosion control will be most cost effective where it is most badly needed. For this reason corrosion control methods that extend the life of the DHE at the waterline and protect it from stray current corrosion are most important. Culver, Lund, and Svanevik (1974) found that the average lifetime of a DHE in Klamath Falls is 14.1 years, with a range from a few years to over 30 years (based on limited data). They report average replacement costs to be approximately $560. If these figures are accurate, there are very few methods of corrosion

control that are economically attractive. Even doubling the life of a DHE has a present value of at most a few hundred dollars. Since stainless steel costs five to ten times as much as mild steel, this means that a stainless steel DHE is prohibitively expensive and even stainless steel would not be entirely free from corrosion. More exotic alloys are even more expensive.

Because of the large variation in life of the DHEs, what is economic for one well may not be for another. For a DHE with a lifetime of fourteen years or more, the economically attractive methods of corrosion control are essentially limited to continued use of steel with protection at the waterline.

In aggressive wells which require frequent replacement of DHEs (say every few years) additional options are available. The entire DHE can be made from stainless steel, though further testing to determine the severity of pitting and crevice corrosion for long exposures would be helpful. Alternately, a much more complete cathodic protection system, as previously discussed, (possibly including the use of an insulating coating over part or all of the DHE to reduce current requirements) could be used.

The following is a summary of recommendations for corrosion control in geothermal wells in Klamath Falls (see Figure 3.4):

(1) Insulating couplings applied at the connection to the DHE to control stray current corrosion.

(2) One or more of the following for wells of average aggressiveness:

(i) a sacrificial anode of magnesium (one or more) attached to the DHE near the waterline and a good electrical connection between the DHE and the casing to cathodically protect the DHE near the waterline.

(ii) a coating of epoxy to isolate the section of DHE near the waterline from the environment.

(iii) a section of stainless steel to replace mild steel in the DHE near the waterline.

(3) In highly aggressive wells, a more complete cathodic protection system or a stainless steel DHE.

4. CONCLUSIONS

Mathematical models of thermosyphoning in cased geothermal wells both with and without a downhole heat exchanger have been developed, and computer programs developed for solution of the resulting equations when necessary.

The thermosyphoning model without DHE shows that thermosyphoning is sufficient to account for observed vertical mass flow rates through the casing.

Results of the thermosyphoning model with the DHE compare favorably with experimental data. Investigations with the model showed that the most promising approaches to maximizing DHE output are the following:

(1) Spacing between perforations should be at least 30 to 40 meters, as output falls off rapidly below this range. Very large spacing should also be avoided.

(2) Use a somewhat smaller than usual casing if possible to allow sufficient flow area between the casing and the wellbore. Too small an area will severly limit output by restricting thermosyphoning through the casing. For a .254m wellbore, the casing should not be larger than .19m if the distance between perforations is large or a single loop is used. If multiple loops are used, the casing should be somewhat larger, especially if the distance between perforations is short.

(3) Slots should be of adequate size.

(4) Both fins and multiple small diameter tubes can lead to a significant increase in output, but the use of multiple tubes has greater potential. The appropriate technique must be decided on an economic basis.

(5) Corrosion control methods, especially in aggressive wells, will tend to keep performance from degrading.

Corrosion and scaling are important considerations in any geothermal system and become more important as attempts are made to maximize DHE output. Aqueous corrosion and corrosion control methods were investigated and methods suitable for controlling corrosion in geothermal wells at Klamath Falls were presented.

The aggressiveness of the wells varies considerably and the best approach is dictated by the severity of the environment. For a moderately corrosive well, the most promising approach consists of electrical isolation of the DHE to control stray current corrosion and local protection in the vicinity of the waterline by the use of a sacrificial anode and epoxy coating, or a section of more corrosion resistant material such as stainless steel. Conditions at the waterline are considerably more corrosive than elsewhere.

In aggressive wells, electrical isolation of the DHE is again called for to control stray current corrosion, and a complete cathodic protection system or stainless steel construction.

Scaling is not perceived to be severe enough to justify the use of available technology for scaling prevention and removal. Corrosion control measures may decrease scaling somewhat by reducing the number of nucleation sites for scaling and minimizing the chemical changes due to corrosion which increase scaling.

Although no detailed economic analysis is included in this work, possible solutions which are clearly uneconomic have not been considered in any detail.

BIBLIOGRAPHY

Applegate, L. M., 1960, Cathodic Protection. McGraw-Hill Book Co., NY.

Banov, A., 1973, Paints and Coatings Handbook, Structures Publishing Co., Farmington, Mich.

Berger, D. M., 1976, "How to Select Coatings for Buried Steel Pipe," Pipeline and Gas Journal, Vol. 203, No. 2, Feb., pp. 14-20.

Burns, R. M., and W. W. Bradley, 1967, Protective Coatings for Metals, 3rd edition, Reinhold Publishing Corp., NY.

Butler, G., and H. C. K. Ison, 1966, Corrosion and its Prevention in Waters, Reinhold Publishing Company, NY.

Churchill, D., G. G. Culver, and G. Reistad, 1977, "Flow Measurement and Characterization in Shallow Geothermal Systems Used for Downhole Heat Exchanger Applications," unpublished.

Culver, G. G., J. W. Lund, and L. S. Svanevik, 1974, "Klamath Falls Hot Water Well Study," UCRL-13614, Lawrence Livermore Laboratory, Livermore, CA.

Cook, F. E., H. S. Preister, and J. F. Mills, 1954, "Electrolytic Descaling," J. American Society of Naval Engineers, Vol. 68, No. 4, Nov., pp. 1005-1050.

Einarsson, S. S., 1961, "Proposed 15mw geothermal power station at Hveragerdi, Iceland," UN Conference on New Sources of Energy, Rome (E/Cont. 35/619). United Nations, NY.

Evans, U. R., 1948, Metallic Corrosion Passivity and Protection, Longmans, Green and Co., NY.

Evans, U. R., 1969, The Corrosion and Oxidation of Metals: Scientific Principles and Practical Applications, Edward Arnold LTD, London.

Ewing, L. W., 1948, in H. H. Uhlig, editor, Corrosion Handbook, Wiley, NY.

Fontana, M. G., and N. D. Greene, 1967, Corrosion Engineering, McGraw Hill, NY.

Fukuda, M., D. B. Kreitlow, G. G. Culver, and G. M. Reistad, 1977, "Natural Convection Heat Transfer Models for Downhole Heat Exchanger Applications in Shallow Geothermal Systems," ASME Paper No. 77-HT-55.

Hamner, N. E., 1970, "Coatings for Corrosion Protection," in NACE Basic Corrosion Course, A. deS. Brasunas, Editor, National Association of Corrosion Engineers, Houston, Tx.

Himmelblau, D. M., 1972, Applied Nonlinear Programming, McGraw Hill Book Co., NY.

Kern, D. Q., and A. D. Kraus, 1972, Extended Surface Heat Transfer, McGraw Hill Book Co., NY.

Langlier, W. F., 1936, "The Analytical Control of Anticorrosion Water Treatment," Journal of The American Water Works Association, Vol. 28, p. 1500.

Lindal, B., 1974, "Geothermal Energy for Process Use," International Conference on Geothermal Energy for Industrial, Agricultural, Commercial-residential Uses, Oregon Institute of Technology, Klamath Falls, OR.

Lund, J. W., J. F. Silva, G. G. Culver, and P. J. Lienau, 1976, "Corrosion of Downhole Heat Exchangers," Report 76-3, Geo-Heat Utilization Center, Oregon Institute of Technology, Klamath Falls, OR.

Marshall, T., and W. R. Braithwaite, 1973, "Corrosion Control in Geothermal Systems" in Geothermal Energy - Review of Research and Development, H. C. H. Armstrong, Editor, UNESCO, Paris.

Matthews, F. J., 1936, Boiler Feedwater Treatment, Hutchinsons Scientific and Technical Publications, London.

Mortimer, C. E., 1967, Chemistry, A Conceptual Approach, Van Nostrand Reinhold Co., NY.

Newcombe, J. M., 1976, "Maintenance Problems and Solutions in Geothermal Well Plumbing," Geo-Heat Utilization Center Quarterly Bulletin, Apr., 1976, Oregon Institute of Technology, Klamath Falls, OR., pp. 4-6.

Owen, L. B., 1976, "Control of Geothermal Scaling and Corrosion," in Energy and Technology Review, UCRL-52000-76-3, March, 1976, Lawrence Livermore Laboratory, Livermore, CA.

Pourbaix, M., 1974, Atlas of Electrochemical Equilibria in Aqueous Solutions, National Association of Corrosion Engineers, Houston, TX.

Reid, R. L., J. S. Tennent, and K. W. Childs, 1975, "The Modelling of a Thermosyphon Type Permafrost Protection Device," ASME Transactions, Vol. 97, Series C., No. 3.

Roberts, S. M., and J. S. Shipman, 1972, Two-Point Boundary Value Problems: Shooting Methods, American Elsevier, NY.

Sass, J. H. and E. A. Sammel, 1976, "Heat Flow Data and Their Relation to Observed Geothermal Phenomena Near Klamath Falls, Oregon," Journal of Geophysical Research, Vol. 21, No. 26.

Scully, J. C., 1975, The Fundamentals of Corrosion, 2nd Edition, Pergammon Press, NY.

Shreir, L. L., 1963, Corrosion, 1st Edition, Wiley, NY.

Shreir, L. L., 1976, Corrosion, 2nd Edition, Butterworth, Inc.

Taborek, J., T. Aoki, R. B. Ritter, J. W. Palen, and J. G. Knudsen, 1972, "Fouling: The Major Unresolved Problem in Heat Transfer, Parts I and II," Chemical Engineering Progress, Vol. 68, No. 2, pp. 59-67; No. 7, pp. 69-78.

Thiruvengadam, A. O., 1976, "Cavitation Descaling Techniques for Geothermal Applications," report COO-2607-4, National Technical Information Service, Springfield, VA.

Tolivia, E., 1970, "Corrosion Measurements in a Geothermal Environment," UN Symposium on the Development and Utilization of Geothermal Resources, Pisa, Vol. 2, part 2, pp. 1596-1601.

Uhlig, H. H., 1948, editor, Corrosion Handbook, Wiley, NY.

Uhlig, H. H., 1963, Corrosion and Corrosion Control, Wiley, NY.

Welty, J. R., C. E. Wicks, and R. E. Wilson, 1969, Fundamentals of Momentum, Heat and Mass Transfer, Wiley, NY.

APPENDIX A

Computer program to solve the

differential equation model with DHE

This program solves the differential equations in chapter 2. The program is designed to be run interactively from a time-sharing terminal. The results of the program are written onto tape6. Intermediate results are written onto tape 7 in order to check convergence.

```
      PROGRAM MAIN(INPUT,OUTPUT,TAPE6,TAPE61=OUTPUT)
      IMPLICIT REAL (M)
      COMMON/B/MDOTH,TIN,THB,MDOT,TCB
      COMMON/ONE/X(2),Y(2),S(2),FX,FY
      COMMON/PR/IP,ITMAX
      COMMON/TST/IFLAG2,CONVT
C
C          THIS PROGRAM SOLVES THE TWO-POINT BOUNDARY VALUE
C          PROBLEM OF A DOWNHOLE HEAT EXCHANGER IN A
C          GEOTHERMAL WELL.  THE DOWNHOLE HEAT EXCHANGER
C          CONSISTS OF  U SHAPED PIECE(S) OF PIPE.  FINS MAY
C          BE ADDED TO THE HEAT EXCHANGER IF DESIRED.
C
C          THE SOLUTION TECHNIQUE USED IS A SHOOTING METHOD
C          ADJUSTING ASSUMED INITIAL CONDITIONS UNTIL THE
C          BOUNDARY VALUES ARE SUFFICIENTLY WELL SATISFIED.
C          A NONLINEAR PROGRAMMING ROUTINE, SUBROUTINE PWL,
C          WHICH USES POWELL'S METHOD, IS USED TO ADJUST THE
C          INITIAL VALUE GUESSES.  THE USER MUST SUPPLY THE
C          INITIAL GUESSES.
C          IF THE INITIAL GUESSES ARE NOT SUFFICIENTLY ACCURATE,
C          THE PROCEDURE MAY FAIL TO CONVERGE, OR
C          CONVERGENCE MAY BE VERY SLOW.
C
C          TOLERANCES USED IN CHECKING FOR CONVERGENCE SHOULD NOT
C          BE TOO SMALL AS EXCESSIVE COMPUTATION TIME MAY BE REQUIRED.
C
C
C
    5 CONTINUE
C
C          IP=PRINT OPTION.  IF IP=1, THE TEMPERATURE
C          PROFILE IS PRINTED.
C
      IP=0
C          CONVT IS USED TO TEST FOR CONVERGENCE.
C
      CONVT=0.1
C
C          READ1 READS THE DATA
C
      CALL READ1
      X(1)=TOB
      X(2)=THB
C
C          ITMAX LIMITS THE NUMBER OF FUNCTION EVALUATIONS
C
      ITMAX=250
C
C
C          SUBROUTINE PWL IS A NONLINEAR PROGRAMMING ROUTINE
C          WHICH IS USED TO SATISFY THE BOUNDARY
C          CONDITIONS.
C
      CALL PWL
      X(1)=TOB
      X(2)=THB
      PRINT*,' MDOT= ',MDOT
      IP=1
C
C         SUBROUTINE OUTPUT1 WRITES THE RESULTS ON TAPE6
C
      CALL OUTPUT1
```

```
      WRITE(6,15)
   15 FORMAT(/,T25,'TEMPERATURE PROFILE',/)
      WRITE(6,16)
   16 FORMAT(1X,'DISTANCE',6X,'TC',9X,'TI',10X,'TH1',9X,'TH2')
      PRINT*,' X(1)= ',X(1),' X(2)= ',X(2)
C
C          SUBROUTINE FUN IS CALLED AGAIN WITH THE PRINT OPTION IN
C          EFFECT SO THAT THE TEMPERATURE PROFILE CAN BE WRITTEN
C          ON  TAPE6.
C
C
      CALL FUN(X,F)
      STOP
      END
C
C
      SUBROUTINE FUN(XX,F)
      IMPLICIT REAL (A)
      REAL K,L
      DIMENSION XX(2)
      COMMON/A/DO,DI,OP,RLRFC,RLRFI,RLRFH
      COMMON/AA/A,L,DISCOND,DELTAT
      COMMON/B/MOOTH,TIN,THB,MOOT,TCB
      COMMON/C/DEO,DEI,AO,AI,AHE,TN
      COMMON/D/ANU,RHO,K,CP,BETA,G
      COMMON/E/REO,REI,REH,FFC,FFI,FFH
      COMMON/FIN/FN,B,OLN,FEFF
      COMMON/S/SF,SO,FT
      COMMON/H/HO,HI,HH
      COMMON/THREE/NN,NFUNCT,NCRV,ITER,INDIC,IPRNT
      COMMON/V/VO,VI,VHE
      COMMON/W/UW,UI,UH
      COMMON/MN/MOOTMN,TOBMN,THBMN,ERR1MN,ERR2MN,FEASMN,FMN
      COMMON/O/TOUT
      COMMON/ER/IPRINT,ITMAX
      DIMENSION T(4),OT(4)
      DATA ANU,RHO,K,CP,BETA,G/.294E-6,969.,.50,.4205,,7.5E-4,9.81/
      DATA EPS,TB,SCOND,RCOND/.001,100.,47.,.78/
      PI=4.0*ATAN(1.0)
C
C          THIS SUBROUTINE SOLVES THE DIFFERENTIAL EQUATIONS FOR A DOWNHOLE
C          HEAT EXCHANGER.
C
C          NFUNCT COUNTS THE NUMBER OF FUNCTION EVALUATIONS
C
      NFUNCT=NFUNCT+1
      IF(NFUNCT.GT.ITMAX)CALL MAXIT
      TOB=XX(1)
      THB=XX(2)
  150 CONTINUE
C
C          CALCULATE FLOW VELOCITIES
C
      VO=MOOT/(RHO*AO)
      VI=MOOT/(RHO*AI)
      VHE=MOOTH/(RHO*AHE*TN)
C
C          CALCULATE REYNOLDS NUMBERS
C
      REO=DEO*VO/ANU
      REI=DEI*VI/ANU
      REH=OP*VHE/ANU
C
```

```
C          CALCULATE FRICTION FACTORS
C
      FFO=FRF(REO,RLRFO)
      FFI=FRF(REI,RLRFI)
      FFH=FRF(REH,RLRFH)
C
C          CALCULATE HEAT TRANSFER COEFFICIENTS
C
      HO=RHO*CP*VO*ST(FFO)
      UW=1./(1./HO+DO*ALOG(1.+2.*DISCOND/DO)/(2.*RCOND))
      CALL HTCOEF(FFO,FFI,FFH,UI)
C
C          CALCULATE FIN EFFICIENCY
C
C          FEFF=FIN EFFICIENCY
C          SF=AREA OF FIN/UNIT LENGTH
C          SO=AREA WITHOUT FIN/UNIT LENGTH
C
C
      IF(FN.EQ.0.)10,20
   10 EMB=B*SQRT(2.*HI/SCOND/DLN)
      FEFF=TANH(EMB)/EMB
   20 IF(FN.EQ.0.)FEFF=0.
C
C          CALCULATE AREAS AND UH
C
      SF=FN*(2.*B+DLN)
      SO=PI*DP-FN*DLN
      UH=(SF*FEFF+SO)/(HH*PI*DP+SF*FEFF*HI+SO*HI)
      UH=UH*HH*HI
C
C          COMPUTE COEFFICIENTS FOR DIFFERENTIAL EQUATION
C
      C1=UI*PI*DI/CP
      C2=UW*PI*DO/CP
      C3=UH*PI*DP*TN/CP
C
C          PREPARE TO INTEGRATE DIFFERENTIAL EQUATIONS
C
      N=4   $  E=.01   $  H=0.5   $  II=1   $  X=0.
      T(1)=TB   $  T(2)=TOB   $  T(3)=THB   $  T(4)=THB
      TOFSM=0.   $  TOL=T(1)-T(2)
C
C          INTEGRATE DIFFERENTIAL EQUATIONS
C
  200 CONTINUE
C
      DT(1)=-(C2*(T(1)-100.+E*X)+C1*(T(1)-T(2)))/MDOT
      DT(2)=-(C1*(T(1)-T(2))+C3*(T(3)+T(4)-2.*T(2)))/MDOT
      DT(3)=C3*(T(3)-T(2))/MECTH
      DT(4)=C3*(T(2)-T(4))/MECTH
      IF(II.GT.2) GO TO 300
C
      IF(IPRINT .EQ. 0) GO TO 250
C
      CK=IFIX(X/5.)
      IF(ABS(X-5.*CK).GT.1.E-3)GO TO 250
      WRITE(6,13)X,T(1),T(2),T(3),T(4)
   13 FORMAT(1H ,F3.0,4(5X,F7.3))
  250 IF(X.GE.L)GO TO 500
C
C          SUBROUTINE HPCG INTEGRATES THE DIFFERENTIAL EQUATIONS.
C
```

```
  300 CALL HPCG(X,T,DT,N,H,E,II)
      IF(II.GT.2)GO TO 200
C
C          THE FOLLOWING 3 LINES INTEGRATE THE TEMPERATURE DIFFERENCE
C          FOR USE IN FINDING THE HEAD DUE TO BUOYANCY.
C
      TD=T(1)-T(2)
      TDFSM=(TDL+TD)*H/2.+TDFSM
      TDL=TD
      GO TO 200
C
  500 CONTINUE
      TOUT=T(4)
      IF(IPRINT.NE.0)RETURN
      FEAS=0.
      HEAD=RHO*BETA*G*TDFSM
      PLOSF=FFI/(RHO*AI*AI*CEI)+FFO/(RHO*AO*AO*CEO)
      PLOSS=2.*L*PLOSF*MDOT*MDOT
      IF(HEAD .LT. 0.)777,888
C
C          THE HEAD IS NEGATIVE.  ADD PENALTY TO F AND INCREASE
C          MDOT
C
  777 PRINT*,* HEAD NEGATIVE *
      FEAS=100.*(PLOSS+HEAD)**2
      MDOT=2.*MDOT
      GO TO 1000
C
C          THE HEAD IS POSITIVE.  CHECK TO SEE IF HEAD=HEADLOSS.
C          IF IT DOES, RETURN.  OTHERWISE, CHANGE MDOT AND TRY
C          AGAIN.
C
  888 CONTINUE
      MDOTL=MDOT
      MDOT=SQRT(HEAD/(PLOSF*2.*L))
      ERRM=(MDOTL-MDOT)/2.
      IF(ABS(ERRM).LT.EPS)GO TO 1000
      GO TO 150
C
C          CALCULATE VALUE OF F=VALUE OF ERROR
C
 1000 CONTINUE
      ERR1=T(2)-T(1)   $  ERR2=T(3)-TIN
      F=ERR1*ERR1+ERR2*ERR2
      F=F+FEAS
C
C          VALUES ARE PRINTED EVERY 25 ITERATIONS
C
      IF(MOD(NFUNCT,25).EQ.0)1025,1050
 1025 PRINT*,*NFUNCT= *,NFUNCT,* MDOT= *,MDOT,* TOB= *,TOB,* THB= *,
     1THB,* F= *,F
      PRINT*,*  ENTER 1 TO CONTINUE *
      READ*,IC
      IF(IC.NE.1)STOP
 1050 CONTINUE
      FI=F
C
C          STORE MINIMUM VALUES IN CASE A RESTART IS NECESSARY
C
      IF(NFUNCT.EQ.1)GO TO 1200
      IF(F.GT.FMN)RETURN
 1200 FMN=F   $  MDOTMN=MDOT   $  TOBMN=TOB   $  THBMN=THB
      ERR1MN=ERR1   $  ERR2MN=ERR2   $  FEASMN=FEAS
```

```
      RETURN
      END
C
      SUBROUTINE READ1
      IMPLICIT REAL (M)
      REAL K,L
      COMMON/A/DO,DI,DP,RLRFO,RLRFI,RLRFH
      COMMON/AA/A,L,DISCOND,DELTAT
      COMMON/C/DEQ,DEI,AO,AI,AHE,TN
      COMMON/D/ANU,RHO,K,CP,BETA,G
      COMMON/B/MDOTH,TIN,THB,MDOT,TCB
      COMMON/FIN/FN,B,DLN,FEFF
      COMMON/ER/IP
      PI=4.*ATAN(1.)
C
C          THIS SUBROUTINE READS THE DATA INPUT AND INITIAL GUESSES.
C
C          TB= TEMPERATURE OF RESERVOIR
C          TH=CASING THICKNESS
C
C          DO=WELLBORE DIAMETER
C          DI=CASING INSIDE DIAMETER
C          DP=ONE OUTSIDE DIAMETER
C
C          L=LENGTH OF WELL
C
C          RLRFO=D/E FOR OUTER ANNULUS
C          RLRFI=D/E FOR INSIDE CASING
C          RLRFH=D/E FOR HEAT EXCHANGER
C
C          DISCOND=CONDUCTION DISTANCE
C          MDOTH=HEAT EXCHANGER MASS FLOW RATE
C          TIN=HEAT EXCHANGER INLET TEMPERATURE
C          DELTAT=TEMPERATURE DIFFERENCE BETWEEN TOP AND BOTTOM
C                 OF WALL
C
C          FN=NUMBER OF FINS
C          B=LENGTH OF FINS
C          DLN=THICKNESS OF FINS
C
      TB=100.  $  TH=.0079
C
C      READ DATA
C
      PRINT*,' ENTER DO,DI,DHE,L,TN'
      READ*,DO,DI,DP,L,TN
      IF(DO.EQ.0.)STOP
      PRINT*,' RLRFO,RLRFI,RLRFH'
      READ*,RLRFO,RLRFI,RLRFH
      PRINT*,' ENTER DISCOND,MDOTH,TIN,DELTAT'
      READ*,DISCOND,MDOTH,TIN,DELTAT
      PRINT*,' ENTER NUMBER OF FINS,LENGTH,AND THICKNESS'
      READ*,FN,B,DLN
C
C      INITIAL GUESSES
C
C          TOB=TEMPERATURE AT BOTTOM OF WELL INSIDE CASING
C          MDOT=MASS FLOW RATE THROUGH CASING
C          THB=TEMPERATURE  AT THE BOTTOM OF THE ONE LOOP
C
C
      PRINT*,' TOB,MDOT,THB'
      READ*,TOB,MDOT,THB
```

```
C
C          CALCULATE ADDITIONAL PARAMETERS
C
C          A=WALL TEMPERATURE GRADIENT
C          DC=OUTSIDE DIAMETER OF CASING
C          DPI=ONE INSIDE DIAMETER
C          DEO=EQUIVALENT DIAMETER OF OUTER ANNULUS
C          AI=CROSS SECTIONAL AREA INSIDE CASING
C          PEI=PERIMETER INSIDE CASING
C          DEI=EQUIVALENT DIAMETER INSIDE CASING
C          AO=CROSS SECTIONAL AREA OF OUTER ANNULUS
C          AHE=CROSS SECTIONAL AREA INSIDE ONE
C          TN=NUMBER OF ONE LOOPS
C
      A=DELTAT/L   $  DC=DI+TH+TH   $  DPI=DP-.0012   $  DEO=DO-DC
      AI=PI*(DI*DI-2.*TN*DP*DP)/4.-FN*B*DLN*2.*TN
      PEI=PI*(DI+2.*TN*DP)+2.*TN*FN*(2.*B+DLN)
      DEI=4.*AI/PEI
      AO=PI*(DO*DO-DC*DC)/4.
      AHE=PI*DPI*DPI/4.
      RETURN
      END
C
      SUBROUTINE MAXIT
      IMPLICIT REAL (M)
      COMMON/B/MOOTH,TIN,THB,MOOT,TOB
      COMMON/S/SF,SO,F
      COMMON/MN/MOOTMN,TOBMN,THBMN,ERR1MN,ERR2MN,FEASMN,FMN
C
C      THIS SUBROUTINE GIVES THE RESULTS AT THE POINT
C      AT WHICH EXECUTION IS TERMINATED IF THE ITERATION
C      LIMIT IS EXCEEDED
C
      PRINT*,' EXCEEDED ITMAX ITERATIONS.  LAST VALUES:'
      PRINT*,' MOOT= ',MOOT,' TOB= ',TOB,' THB= ',THB
      PRINT*,' FUNCTION VALUE= ',F
      PRINT*,' BEST VALUE:  F= ',FMN
      PRINT*,' MOOT= ',MOOTMN,' TOB= ',TOBMN,' THB= ',THBMN
      STOP
      END
C
C
      FUNCTION ST(FF)
C
C          THIS FUNCTION COMPUTES THE STANTON NUMBER BY
C          THE PRANDTL ANALOGY
C
      PR=1.75
      CF2=FF/2.
      ST=CF2/(1.0+5.0*SQRT(CF2)*(PR-1.0))
      RETURN
      END
C
C
      SUBROUTINE HTCOEF(FFO,FFI,FFH,UI)
      COMMON/V/VO,VI,VHE
      COMMON/C/ANU,RHO,K,CP,BETA,G
      COMMON /H/HO,HI,HH
      COMMON/W/UW
C
C          THIS SUBROUTINE CALCULATES HEAT TRANSFER COEFFICIENTS
C          AND THE OVERALL HEAT TRANSFER COEFFICIENT THROUGH THE
C          CASING, UI.
```

```
C
      HI=RHO*CP*VI*ST(FFI)
C          NOTE-CASING THICKNESS IGNORED
      UI=HO*HI/(HO+HI)
      HH=RHO*CP*VHE*ST(FFH)
      RETURN
      END
C
      FUNCTION FRF(RE,RLRF)
C
C          FUNCTION FRF DETERMINES THE FRICTION FACTOR
C                THE EQUATIONS USED ARE FROM WELTY,WICKS AND WILSON
C                CHAPTER 14.
C
      FF=.01
      I=1
      IF(RE.LT.2300.)GO TO 300
      IF(RE.GT.1.E7)GO TO 200
C
C          TRANSITION REGION
C
   10 FN=4.*ALOG10(RLRF)+2.28-4.*ALOG10(4.67*RLRF/(RE*SQRT(FF)))+1.0)
      FN=1./(FN*FN)
      IF(ABS(FN-FF).LT.1.E-5) GO TO 100
      I=I+1
      FF=FN
      IF(I.LT.100)GO TO 10
      PRINT*,' FRF FAILS TO CONVERGE'
      STOP
  100 IF(RLRF/(RE*SQRT(FF)).GT..01)GO TO 400
  200 FF=1.0/(4.*ALOG10(RLRF)+2.28)**2
      GO TO 400
  300 FF=16./RE
  400 FRF=FF
      RETURN
      END
C
      SUBROUTINE OUTPUT1
      IMPLICIT REAL (M)
      REAL K,L
      COMMON/A/DO,DI,DP,RLRFO,RLRFI,RLRFM
      COMMON/AA/A,L,DISCOND,DELTAT
      COMMON/B/MOOTH,TIN,THB,MOOT,TCB
      COMMON/C/DFO,DFI,AO,AI,AHE,TN
      COMMON/D/ANU,RHO,K,CP,BETA,G
      COMMON/E/REO,REI,REH,FFO,FFI,FFM
      COMMON/FIN/FN,B,DLN,FEFF
      COMMON/H/HO,HI,HH
      COMMON/V/VO,VI,VHE
      COMMON/W/UW,UI,UH
      COMMON/O/TOUT
C
C       WRITE RESULTS ON FILE
C
      WRITE(6,501)
      EN=CP*MOOTH*(TOUT-TIN)
  501 FORMAT(1H1,/////,T30,' WELL CHARACTERISTICS',/)
      WRITE(6,502)L,DISCOND
  502 FORMAT(T15,'LENGTH=',F5.1,' METERS',5X,' COND DISTANCE= ',
     1F7.3,' METERS')
      IFN=FN     $   NT=TN
      WRITE(6,511)IFN,B,DLN,FEFF
  511 FORMAT(T15,'NUMBER OF FINS= ',I2,'  LENGTH= ',F6.4,' THICKNESS= '
```

```
     1,F6.5,' EFFICIENCY= ',F5.3)
      WRITE(6,509)DELTAT
  509 FORMAT(T15,'WALL TEMP (BOTTOM-TOP)= ',F7.3,' DEGREES C')
      WRITE(6,503)MDOTH,TIN,NT
  503 FORMAT(/,T15,'MDOTH= ',F5.2,' KG/SEC',4X,' INLET TEMP= ',
     1F6.2,' DEGREES C',4X,I2,' ONE LOOPS')
      WRITE(6,504)MDOT,EN
  504 FORMAT(T15,'MASS FLOW RATE= ',F5.2,' KG/S',/,T15,'ENERGY RATE= ',
     1E10.4,' WATTS')
      WRITE(6,505)
  505 FORMAT(/,T18,3HDIA,7X,3HD/E,8X,2HFF,8X,1HV,9X,2HRE,9X,1HH,
     19X,1HU)
      WRITE(6,506)DI,RLRFI,FFI,VI,REI,HI,UI
  506 FORMAT(T5,' INSIDE',T17,F6.4,4X,F5.0,5X,F6.5,4X,F5.3,4X,E8.2,
     13X,F6.0,4X,F6.1)
      WRITE(6,507)DO,RLRFO,FFO,VO,REO,HO,UW
  507 FORMAT(T5,' OUTSIDE',T17,F6.4,4X,F5.0,5X,F6.5,4X,F5.3,4X,E8.2,
     13X,F6.0,4X,F6.1)
      WRITE(6,508)DP,RLRFH,FFH,VHE,REH,HH,UH
  508 FORMAT(T5,' HT EXCH',T17,F6.4,4X,F5.0,5X,F6.5,4X,F5.3,4X,E8.2,
     13X,F6.0,4X,F6.0)
      RETURN
      END
C
C
      SUBROUTINE HPCG(X,Y,DERY,NDIM,H,ERR,II)
      DIMENSION Y(NDIM),DERY(NDIM),AUX(16,20)
C
C          THIS SUBROUTINE SOLVES DIFFERENTIAL EQUATIONS BY USING
C          A MODIFIED HAMMING'S METHOD.
C
      GO TO(501,24,503,504,505,506,507,508,509,510,511),II
  501 X0=X
      DIM=1./FLOAT(NDIM)
      M=1
      IHLF=0
      DO 1 I=1,NDIM
      AUX(16,I)=0.
      AUX(15,I)=DIM
      AUX(8,I)=DERY(I)
    1 AUX(1,I)=Y(I)
C
C     COMPUTATION OF AUX(2,I)
      ISW=1
      GOTO 100
C
    9 X=X+H
      DO 10 I=1,NDIM
   10 AUX(2,I)=Y(I)
C
C     INCREMENT H IS TESTED BY MEANS OF BISECTION
   11 IHLF=IHLF+1
      X=X-H
      DO 12 I=1,NDIM
   12 AUX(4,I)=AUX(2,I)
      H=.5*H
      M=1
      ISW=2
      GOTO 100
C
   13 X=X+H
      II=6
      RETURN
```

```
  506 M=2
      DO 14 I=1,NDIM
      AUX(2,I)=Y(I)
   14 AUX(9,I)=DERY(I)
      ISW=3
      GOTO 100
C
C     COMPUTATION OF TEST VALUE DELT.
   15 DELT=0.
      DO 16 I=1,NDIM
   16 DELT=DELT+AUX(15,I)*ABS(Y(I)-AUX(4,I))
      DELT=.06666667*DELT
      IF(DELT-ERR     )19,19,17
   17 IF(IHLF-10)11,18,18
C
C     NO SATISFACTORY ACCURACY AFTER 10 BISECTIONS. ERROR MESSAGE.
   18 WRITE(61,1000)
 1000 FORMAT (1X,*ERROR  10 BISECTIONS OF STEP  WERE INSUFFICIENT*)
      STOP
C
C     THERE IS SATISFACTORY ACCURACY AFTER LESS THAN 11 BISECTIONS.
   19 X=X+H
      II=7
      RETURN
  507 DO 20 I=1,NDIM
      AUX(3,I)=Y(I)
   20 AUX(10,I)=DERY(I)
      M=3
      ISW=4
      GOTO 100
C
   21 M=1
      X=X+H
      II=8
      RETURN
  508 X=X0
      DO 22 I=1,NDIM
      AUX(11,I)=DERY(I)
   22 Y(I)=AUX(1,I)+H*(.375*AUX(8,I)+.7916667*AUX(9,I)
     1-.2083333*AUX(10,I)+.04166667*DERY(I))
   23 X=X+H
      M=M+1
      II=2
      RETURN
   24 IF (M-4 ) 25,200,211
   25 DO 26 I=1,NDIM
      AUX(M,I)=Y(I)
   26 AUX(M+7,I)=DERY(I)
      IF(M-3)27,29,200
C
   27 DO 28 I=1,NDIM
      DELT=AUX(9,I)+AUX(9,I)
      DELT=DELT+DELT
   28 Y(I)=AUX(1,I)+.3333333*H*(AUX(8,I)+DELT+AUX(10,I))
      GOTO 23
C
   29 DO 30 I=1,NDIM
      DELT=AUX(9,I)+AUX(10,I)
      DELT=DELT+DELT+DELT
   30 Y(I)=AUX(1,I)+.375*H*(AUX(8,I)+DELT+AUX(11,I))
      GOTO 23
C
C     THE FOLLOWING PART OF SUBROUTINE HPCG COMPUTES BY MEANS OF
```

```
C     RUNGE-KUTTA METHOD STARTING VALUES FOR THE NOT SELF-STARTING
C     PREDICTOR-CORRECTOR METHOD.
  100 DO 101 I=1,NOIM
      Z=H*AUX(M+7,I)
      AUX(5,I)=Z
  101 Y(I)=AUX(M,I)+.4*Z
C     Z IS AN AUXILIARY STORAGE LOCATION
C
      Z=X+.4*H
      II=3
      RETURN
  503 DO 102 I=1,NOIM
      Z=H*DERY(I)
      AUX(6,I)=Z
  102 Y(I)=AUX(M,I)+.2969776*AUX(5,I)+.1587596*Z
C
      Z=X+.4557372*H
      II=4
      RETURN
  504 DO 103 I=1,NOIM
      Z=H*DERY(I)
      AUX(7,I)=Z
  103 Y(I)=AUX(M,I)+.2181004*AUX(5,I)-3.050965*AUX(6,I)+3.832665*Z
C
      Z=X+H
      II=5
      RETURN
  505 DO 104 I=1,NOIM
  104 Y(I)=AUX(M,I)+.1747603*AUX(5,I)-.5514507*AUX(6,I)
     1+1.205536*AUX(7,I)+.1711848*H*DERY(I)
      GOTO(9,13,15,21),ISW
C
C     POSSIBLE BREAK-POINT FOR LINKAGE
C
C     STARTING VALUES ARE COMPUTED.
C     NOW START HAMMINGS MODIFIED PREDICTOR-CORRECTOR METHOD.
  200 N=M
      ISTEP=3
  201 IF(N-8)204,202,204
C
C     N=8 CAUSES THE ROWS OF AUX TO CHANGE THEIR STORAGE LOCATIONS
  202 DO 203 N=2,7
      DO 203 I=1,NOIM
      AUX(N-1,I)=AUX(N,I)
  203 AUX(N+6,I)=AUX(N+7,I)
      N=7
C
C     N LESS THAN 8 CAUSES N+1 TO GET N
  204 N=N+1
C
C     COMPUTATION OF NEXT VECTOR Y
      DO 205 I=1,NOIM
      AUX(N-1,I)=Y(I)
  205 AUX(N+6,I)=DERY(I)
      X=X+H
  206 ISTEP=ISTEP+1
      DO 207 I=1,NOIM
     0DELT=AUX(N-4,I)+1.333333*H*(2AUX(N+6,I)+AUX(N+6,I)-AUX(N+5,I)+
     1AUX(N+4,I)+AUX(N+4,I))
      Y(I)=DELT-.9256198*AUX(16,I)
  207 AUX(16,I)=DELT
C     PREDICTOR IS NOW GENERATED IN ROW 16 OF AUX, MODIFIED PREDICTOR
C     IS GENERATED IN Y. DELT MEANS AN AUXILIARY STORAGE.
```

```
C
      II=9
      RETURN
C     DERIVATIVE OF MODIFIED PREDICTOR IS GENERATED IN DERY
C
  509 DO 208 I=1,NDIM
     0DELT=.125*(9.*AUX(N-1,I)-AUX(N-3,I)+3.*H*(DERY(I)+AUX(N+6,I)+
     1AUX(N+6,I)-AUX(N+5,I)))
      AUX(16,I)=AUX(16,I)-DELT
  208 Y(I)=DELT+.07478017*AUX(16,I)
C
C     TEST WHETHER H MUST BE HALVED OR DOUBLED
      DELT=0.
      DO 209 I=1,NDIM
  209 DELT=DELT+AUX(15,I)*ABS(AUX(16,I))
      IF(DELT-ERR    )210,222,222
C
C     H MUST NOT BE HALVED. THAT MEANS Y(I) ARE GOOD.
  210 II=2
      N=5
      RETURN
  211 IF(IHLF-11)215,18,18
  215 IF(DELT-.02*ERR    )216,216,201
C
C
C     H COULD BE DOUBLED IF ALL NECESSARY PRECEEDING VALUES ARE
C     AVAILABLE
  216 IF(IHLF)201,201,217
  217 IF(N-7)201,218,218
  218 IF(ISTEP-4)201,219,219
  219 IMOD=ISTEP/2
      IF(ISTEP-IMOD-IMOD)201,220,201
  220 H=H+H
      IHLF=IHLF-1
      ISTEP=0
      DO 221 I=1,NDIM
      AUX(N-1,I)=AUX(N-2,I)
      AUX(N-2,I)=AUX(N-4,I)
      AUX(N-3,I)=AUX(N-6,I)
      AUX(N+6,I)=AUX(N+5,I)
      AUX(N+5,I)=AUX(N+3,I)
      AUX(N+4,I)=AUX(N+1,I)
      DELT=AUX(N+6,I)+AUX(N+5,I)
      DELT=DELT+DELT+DELT
  221 AUX(16,I)=8.962963*(Y(I)-AUX(N-3,I))-3.361111*H*(DERY(I)+DELT
     1+AUX(N+4,I))
      GOTO 201
C
C
C     H MUST BE HALVED
  222 IHLF=IHLF+1
      IF(IHLF-10)223,223,210
  223 H=.5*H
      ISTEP=0
      DO 224 I=1,NDIM
     0Y(I)=.00390625*(80.*AUX(N-1,I)+135.*AUX(N-2,I)+40.*AUX(N-3,I)+
     1AUX(N-4,I))-.1171875*(AUX(N+6,I)-6.*AUX(N+5,I)-AUX(N+4,I))*H
     0AUX(N-4,I)=.00390625*(12.*AUX(N-1,I)+135.*AUX(N-2,I)+
     1109.*AUX(N-3,I)+AUX(N-4,I))-.0234375*(AUX(N+6,I)+19.*AUX(N+5,I)-
     29.*AUX(N+4,I))*H
      AUX(N-3,I)=AUX(N-2,I)
  224 AUX(N+4,I)=AUX(N+5,I)
      X=X-H
```

```
      DELT=X-(H+H)
      II=10
      RETURN
  510 DO 225 I=1,NOIM
      AUX(N-2,I)=Y(I)
      AUX(N+5,I)=OERY(I)
  225 Y(I)=AUX(N-4,I)
      DELT=DELT-(H+H)
      II=11
      RETURN
  511 DO 226 I=1,NOIM
      DELT=AUX(N+5,I)+AUX(N+4,I)
      DELT=DELT+DELT+DELT
     0AUX(16,I)=8.962963*(ALX(N-1,I)-Y(I))-3.361111*H*(AUX(N+6,I)+DELT
     1+OERY(I))
  226 AUX(N+3,I)=OERY(I)
      GOTO 206
      END
C
C
      SUBROUTINE PWL
      COMMON/ONE/X(2),Y(2),S(2),FX,FY
      COMMON/TWO/DIRECT(2,2),CUM(2),BEFORE(2),FIRST(2)
      COMMON/THREE/N,NFUNCT,NCRV,ITER,INDIC,IPRINT
      COMMON/TST/IFLAG2,CONVT
      COMMON/MN/MOOTMN,TOEMN,THBMN,ERR1MN,ERR2MN,FEASMN
      DIMENSION W(2),SECND(2)
C
C          THIS SUBROUTINE IS A NONLINEAR PROGRAMMING ROUTINE USING
C          POWELLS METHOD.  IT IS ADAPTED FROM HIMMELBLAU
C          *APPLIED NONLINEAR PROGRAMMING*.
C
      IPRINT=1
      ACC=.001
      N=2
      ICONVG=1
      STEP=.5
C
C          THIS PROGRAM USES POWELLS METHODS FOR DETERMINING THE
C          MINIMUM OF A NONLINEAR FUNCTION OF N VARIABLES.
C
C     DESCRIPTION OF PARAMETERS
C          N= NUMBER OF VARIABLES
C          STEP=INITIAL STEP SIZE
C          ACC= REQUIRED ACCURACY IN FUNCTION AND VARIABLE VALUES
C          IPRINT= PRINT OPTION.  IPRINT=1 GIVES COMPLETE OUTPUT,
C               IPRINT=2 GIVES FINAL RESULT ONLY.
C          NFUNCT=THE NUMBER OF FUNCTION EVALUATIONS
C
C          X IS THE ARRAY REPRESENTING THE PARAMETERS TO BE
C          VARIED.   PWL MUST BE ENTERED WITH AN INITIAL ESTIMATE
C         ESTIMATE IN X.
C
      INDIC=2  $  IFLAG2=0  ¢  NFUNCT=0  ¢  ITER=0  $  N1=N-1
      STEPA=STEP
C
C          SET UP THE INITIAL DIRECTION MATRIX USING UNIT VECTORS
C
   71 CONTINUE
      DO 2 I=1,N
      DO 1 J=1,N
      DIRECT(J,I)=0.
    1 CONTINUE
```

```
      DIRECT(I,I)=1.
    2 CONTINUE
C
C          EVALUATE THE FUNCTION AT THE INITIAL VARIABLE VALUES
C
  100 CALL FUN(X,FX)
      IF(FX.LT.CONVT)RETURN
      PRINT 2000,ITER,NFUNCT,FX
 2000 FORMAT(' ITER= ',I5,2X,' NFUNCT= ',I5,2X,' FX= ',F10.5)
      PRINT*,(X(I),I=1,N)
      GO TO 301
C
C          SAVE THE FINAL FUNCTION VALUE (F1) AND THE FINAL VARIABLE
C          VALUES (BEFORE) FROM THE PREVIOUS CYCLE.
C
    3 CONTINUE
      ITER=ITER+1
      IF(IPRINT .EQ. 1) PRINT 2000,ITER,NFUNCT,FX
      IF(IPRINT .EQ. 1) PRINT*,(X(I),I=1,N)
  301 F1=FX
      DO 4 I=1,N
      BEFORE(I)=X(I)
    4 CONTINUE
      SUM=0.
C
C          AT THE END OF THE CYCLE, SUM WILL CONTAIN THE MAXIMUM CHANGE
C          IN THE FUNCTION VALUE FOR ANY SEARCH DIRECTION, AND ISAVE
C          INDICATES THE DIRECTION VECTOR TO WHICH IT CORRESPONDS.
C
      DO 9 I=1,N
      DO 5 J=1,N
C
C          S CONTAINS THE INITIAL STEP SIZES IN THE I-TH DIRECTION
C
      S(J)=DIRECT(J,I)*STEP
    5 CONTINUE
C
C          FIND THE MINIMUM IN THE ITH DIRECTION, AND THE CHANGE IN
C          FUNCTION VALUE.
C
      CALL SEARCH
      IF(IFLAG2.NE.0)RETURN
      A=FX-FY
      IF(A-SUM)7,7,6
    6 CONTINUE
      ISAVE=I
      SUM=A
C
C          TRANSFER THE NEW FUNCTION AND VARIABLE VALUES TO FX AND X
C
    7 DO 8 J=1,N
      X(J)=Y(J)
    8 CONTINUE
      FX=FY
    9 CONTINUE
C
C          NOW INVESTIGATE WHETHER A NEW SEARCH DIRECTION SHOULD BE
C          INCORPORATED INSTEAD OF THE ISAVE DIRECTION.
C
      F2=FX
      DO 10 I=1,N
      W(I)=2.*X(I)-BEFORE(I)
   10 CONTINUE
```

```
      CALL FUN(W,F3)
      IF(F3.LT.CONVT)RETURN
      A=F3-F1
      IF(A)11,19,19
   11 CONTINUE
      A=2.*(F1-2.*F2+F3)*((F1-F2-SUM)/A)**2
      IF(A-SUM)12,19,19
C
C          A NEW SEARCH DIRECTION IS REQUIRED. FIRST REMOVE ROW ISAVE.
C
   12 CONTINUE
      IF(ISAVE-N)13,15,15
   13 DO 14 I=ISAVE,N1
      II=I+1
      DO 14 J=1,N
      DIRECT(J,I)=DIRECT(J,II)
   14 CONTINUE
C
C          SET THE NTH DIRECTION VECTOR EQUAL TO THE NORMALISED
C          DIFFERENCE BETWEEN THE INITIAL AND FINAL VARIABLE VALUES
C          FOR LAST CYCLE.
C
   15 CONTINUE
      A=0.
      DO 16 J=1,N
      DIRECT(J,N)=X(J)-BEFORE(J)
      A=DIRECT(J,N)**2+A
   16 CONTINUE
      A1=A
      A=1./SQRT(A1)
      DO 17 J=1,N
      DIRECT(J,N)=DIRECT(J,N)*A
      S(J)=DIRECT(J,N)*STEP
   17 CONTINUE
      CALL SEARCH
      IF(IFLAG2.NE.0)RETURN
      FX=FY
      DO 18 I=1,N
      X(I)=Y(I)
   18 CONTINUE
C
C          TEST FOR CONVERGENCE
C
   19 CALL TEST(F1,FX,BEFORE,X,FLAG,N,ACC)
      IF(FLAG)22,500,20
C
C          CONVERGENCE NOT YET ACHEIVED. COMPUTE A NEW STEP SIZE
C          AND GO BACK TO 3
C
   20 IF(F1-FX)121,120,120
  121 CONTINUE
      STEP=-.4*SQRT(ABS(F1-FX))
      GO TO 123
  120 CONTINUE
      STEP=.4*SQRT(F1-FX)
  123 CONTINUE
      IF(STEPA-STEP)21,3,3
   21 CONTINUE
      STEP=STEPA
      GO TO 3
C
C
   22 CONTINUE
```

```
      PRINT*,' MINIMUM VALUE OF OBJECTIVE FUNCTION ',FX
      PRINT*, ' VALUES OF INDEPENDENT VARIABLES ',(X(I),I=1,N)
      PRINT*,' NUMBER OF FUNCTION EVALUATIONS ',NFUNCT
      RETURN
C
C          CONVERGENCE HAS STOPPED.  PERTURB BEST SOLUTION AND
C          RUN AGAIN.
C
  500 CONTINUE
      PRINT*,'RESTART NUMBER ',START
      IF(START.GT.4)CALL MAXIT
      IF(ERR1MN.GT.0.)501,502
  501 TOB=TOBMN-.1*START
      GO TO 503
  502 TOB=TOBMN+.1*START
  503 IF(ERR2MN.GT.0.)504,505
  504 THB=THBMN-.05*START
      GO TO 506
  505 THB=THBMN+.05*START
  506 MOOT=MOOTMN-.01
      START=START+1.
      STEPA=STEP
      X(1)=TOB
      X(2)=THB
      GO TO 71
      END
C
      SUBROUTINE TEST(FI,FF,FI,RF,FLAG,N,ACC)
      COMMON/TST/IFLAG2,CONVT
      DATA FL/0.0/
C
C          THIS SUBROUTINE TESTS FOR CONVERGENCE.
C
      FLAG=2.
C
C          IS  THE ERROR SMALLER THAN CONVT.
C
      IF(FF.LT.CONVT)10,20
   10 FLAG=-2.
      FL=0.0
      RETURN
C
C          IS CONVERGENCE PROCEEDING.
C
   20 FD=ABS(FF-FL)
      IF(FD.GT.1.E-4)30,40
   30 FL=FF
      RETURN
   40 FL=0.
      FLAG=0.
      RETURN
      END
C
      SUBROUTINE SEARCH
C
C          THIS SUBROUTINE PERFORMS A ONE-DIMENSIONAL SEARCH
C          IT IS FROM HIMMELBLAU'S 'APPLIED NONLINEAR PROGRAMMING'
C
      COMMON/ONE/X(2),Y(2),S(2),FX,FY
      COMMON/TWO/H(2,2),DELX(2),DELG(2),GX(2)
      COMMON/THREE/N,NFUNCT,NDRV,ITER,INDIC,IPRINT
      COMMON/TST/IFLAG2,CONVT
C
```

```
      IEXIT=0
      NTOL=0
      FTOL=.001
      FTOL2=FTOL/100.
      FA=FB=FC=FX
      DA=DB=DC=0.0
      K=-2
      M=0
      STEP=1.
      D=STEP
C
C           USE THE PARAMETER INDIC TO INDICATE HOW THE SEARCH
C           VECTOR LENGTH SHOULD BE SCALED.
C           INDIC=2 MEANS DO NOT SCALE
C
      IF(INDIC .EQ. 2 .OR. ITER .EQ. 0) GO TO 1
C
C           FIND NORM OF S AND NORM OF DELX
C
      DXNORM=0.
      SNORM=0.
      DO 102 I=1,N
      DXNORM=DXNORM+DELX(I)*DELX(I)
      SNORM=SNORM+S(I)*S(I)
  102 CONTINUE
      IF(INDIC .EQ. 1 .AND. DXNORM .GE. SNORM) GO TO 1
      RATIO=DXNORM/SNORM
      STEP=SQRT(RATIO)
      D=STEP
C
C           START THE SEARCH
C
    1 DO 2 I=1,N
      Y(I)=X(I)+D*S(I)
    2 CONTINUE
      CALL FUN(Y,F)
      IF(F.GT.CONVT)GO TO 211
      IFLAG2=1
      RETURN
  211 CONTINUE
      K=K+1
      IF(F-FA)5,3,6
C
C           NO CHANGE IN FUNCTION VALUE.  RETURN WITH VECTOR
C           CORRESPONDING TO FUNCTION VALUE OF FA, BECAUSE IF THE
C           FUNCTION VALUE IS INDEPENDENT OF THIS SEARCH DIRECTION,
C           THEN CHANGES IN THE VARIABLE VALUES MAY UPSET THE MAIN
C           PROGRAM CONVERGENCE TESTING.
C
    3 DO 4 I=1,N
      Y(I)=X(I)+DA*S(I)
    4 CONTINUE
      FY=FA
      IF(IPRINT .EQ. 1)PRINT 2100
 2100 FORMAT(' SEARCH FAILED.  FUNCTION VALUE INDEP OF D')
      GO TO 326
C
C           THE FUNCTION IS STILL DECREASING.  INCREASE THE STEP
C           SIZE BY DOUBLE THE PREVIOUS INCREASE IN STEP SIZE.
C
    5 CONTINUE
      FC=FB
      FB=FA  $  FA=F
```

```
      OC=OB  $  OB=OA  $  OA=O
      O=2.*O+STEP
      GO TO 1
C
C      MINIMUM IS BOUNDED IN AT LEAST ONE DIRECTION.
C
    6 IF(K)7,8,9
C
C          MINIMUM IS BOUNDED IN ONE DIRECTION ONLY.  REVERSE THE
C          SEARCH DIRECTION AND RECYCLE.
C
    7 CONTINUE
      FB=F  $  OB=O  $  O=-O  $  STEP=-STEP
      GO TO 1
C
C          MINIMUM IS BOUNDED IN BOTH DIRECTIONS AFTER ONLY 2
C          FUNCTION EVALUATIONS.
C          PROCEED TO PARABOLIC INTERPOLATION.
C
    8 FC=FB  $  FB=FA  $  FA=F  $  OC=OB  $  OB=OA  $  OA=O
      GO TO 21
C
C          THE MINIMUM IS BOUNDED AFTER AT LEAST 2 FUNCTION EVALU-
C          ATIONS IN THE SAME DIRECTION.  EVALUATE THE FUNCTION AT
C          STEP SIZE=(OA+OB)/2.  THIS WILL YIELD 4 EQUALLY
C          SPACED POINTS BOUNDING THE MINIMUM.
C
    9 OC=OB
      OB=OA
      OA=O
      FC=FB
      FB=FA
      FA=F
   10 CONTINUE
      O=.5*(OA+OB)
      DO 11 I=1,N
      Y(I)=X(I)+O*S(I)
   11 CONTINUE
      CALL FUN(Y,F)
      IF(F.GT.CONVT)GO TO 213
      IFLAG2=1
      RETURN
  213 CONTINUE
C
C          REMOVE EITHER POINT A OR POINT B IN SUCH A WAY THAT
C          THE FUNCTION IS BOUNDED.
C
   12 IF((OC-O)*(O-OB))15,13,16
C
C          LOCATION OF MINIMUM IS LIMITED BY ROUNDING ERRORS.
C          RETURN WITH 9.
C
   13 DO 14 I=1,N
      Y(I)=X(I)+OB*S(I)
   14 CONTINUE
      FY=FB
      IF(IEXIT .EQ. 1) GO TO 32
      IF(IPRINT .EQ. 1) PRINT 2200
 2200 FORMAT(* SEARCH FAILED.  ROUNDING ERRORS*)
      GO TO 325
C
C          THE POINT O IS IN THE RANGE OA TO OB
C
```

```
   15 IF(F-FB)16,13,17
   16 FC=FB  $  FB=F  $  OC=CB  $  CB=0
      GO TO 21
   17 FA=F  $  OA=0
      GO TO 21
C
C          THE POINT O IS IN THE RANGE OB TO OC
   18 IF(F-FB)19,13,20
   19 FA=FB
      FB=F
      OA=OB
      OB=0
      GO TO 21
   20 FC=F
      OC=0
C
C          NOW PERFORM THE PARABOLIC INTERPOLATION.
C
   21 CONTINUE
      A=FA*(OB-OC)+FB*(OC-OA)+FC*(OA-OB)
      IF(A)22,30,22
   22 CONTINUE
      O=.5*((OB*OB-OC*OC)*FA+(OC*OC-OA*OA)*FB+(OA*OA-OB*OB)*FC)/A
C
C          CHECK TO SEE IF POINT IS GOOD
C          IF SO, EVALUATE THE FUNCTION.
C
      IF((OA-O)*(O-OC))13,13,23
   23 DO 24 I=1,N
      Y(I)=X(I)+O*S(I)
   24 CONTINUE
      CALL FUN(Y,F)
      IF(F.GT.CONVT)GO TO 214
      IFLAG2=1
      RETURN
  214 CONTINUE
C
C          CHECK FOR CONVERGENCE
C
      IF(ABS(FB)-FTOL2)25,25,26
   25 CONTINUE
      A=1.
      GO TO 27
   26 CONTINUE
      A=1./FB
   27 CONTINUE
      IF((ABS(FB-F)*A)-FTOL)28,28,12
C
C          CONVERGENCE ACHEIVED.  RETURN WITH THE SMALLER OF F
C          AND FB.
C
   28 IEXIT=1
      IF(F-FB)29,13,13
   29 FY=F
      GO TO 32
C
C          THE PARABOLIC INTERPOLATION WAS PREVENTED BY THE DIVISOR
C          BEING ZERO.  IF THIS IS THE FIRST TIME THAT IT HAS
C          HAPPENED, TRY AN INTERMEDIATE STEP SIZE AND RECYCLE,
C          OTHERWISE GIVE UP.
C
   30 IF(M)31,31,13
   31 CONTINUE
```

```
      M=M+1
      GO TO 10
   32 DO 99 I=1,N
      IF(Y(I).NE.X(I)) GO TO 325
   99 CONTINUE
      GO TO 33
  325 IF(NTOL .NE. 0 .AND. IPRINT .EQ. 1) PRINT 3000,NTOL
 3000 FORMAT(/ TOLERANCE REDUCED /,I2,2X,/ TIMES/)
  326 IF(FY.LT.FX)RETURN
      IF(S(1) .NE. -GX(1) .OR. (FY .LT. FX)) RETURN
      PRINT*,/ SEARCH FAILED/
      PRINT*,/ VALUE OF OBJECTIVE FUNCTION /,FX
      PRINT*,/ VALUES OF INDEPENDENT VARIABLES /,(X(I),I=1,N)
      PRINT*,/ NUMBER OF FUNCTION EVALUATIONS /,NFUNCT
      STOP
   33 IF(NTOL .EQ. 5) GO TO 34
      IEXIT=0
      NTOL=NTOL+1
      FTOL=FTOL/10.
      GO TO 12
   34 IF(IPRINT .EQ. 1) PRINT*,/ BETTER POINT NOT FOUND/
      RETURN
      END
```